Vacuum polarization for lukewarm black holes

Elizabeth Winstanley[*] and Phil M. Young

Department of Applied Mathematics, The University of Sheffield, Hicks Building, Hounsfield Road, Sheffield, S3 7RH, United Kingdom
(Received 27 September 2007; published 8 January 2008)

We compute the renormalized expectation value of the square of a quantum scalar field on a Reissner-Nordström−de Sitter black hole in which the temperatures of the event and cosmological horizons are equal ("lukewarm" black hole). Our numerical calculations for a thermal state at the same temperature as the two horizons indicate that this renormalized expectation value is regular on both the event and cosmological horizons. We are able to show analytically, using an approximation for the field modes near the horizons, that this is indeed the case.

I. INTRODUCTION

The renormalized stress-energy tensor (RSET) $\langle T_{\mu\nu} \rangle_{\text{ren}}$ is an object of fundamental importance in quantum field theory in curved space-time, since it governs, via the semiclassical Einstein equations

$$G_{\mu\nu} = 8\pi G \langle T_{\mu\nu} \rangle_{\text{ren}},$$

the backreaction of the quantum field on the space-time geometry. Computing the RSET on a particular space-time background is a complicated process [1–4], and, for a quantum scalar field ϕ, it is informative to study first the renormalized vacuum polarization $\langle \phi^2 \rangle_{\text{ren}}$, which is considerably easier to compute and has many of the same features as the full RSET. For example, although $\langle \phi^2 \rangle_{\text{ren}}$ is a scalar object and hence cannot distinguish between future and past event horizons, nonetheless, if it diverges at a horizon for a particular quantum state, then it is likely that the RSET also diverges there.

The vacuum polarization $\langle \phi^2 \rangle_{\text{ren}}$ has been extensively studied by many authors for various black hole backgrounds, beginning with computations by Candelas [5] of $\langle \phi^2 \rangle_{\text{ren}}$ for a massless, conformally coupled, scalar field on the event horizon (and at infinity) for a Schwarzschild black hole. This was subsequently extended to the whole of the Schwarzschild geometry in Refs. [6] (exterior to the event horizon) and [7] (interior to the event horizon). The corresponding calculation for massive scalar fields was done by Anderson [8]. Other examples of calculations of $\langle \phi^2 \rangle_{\text{ren}}$ on more general black hole space-times can be found in [9]. As well as exact, numerical calculations, a number of approximation schemes have been developed for various types of space-times, both for $\langle \phi^2 \rangle_{\text{ren}}$ [10] and the RSET [11].

Of the three standard vacua for quantum fields on black hole space-times (Hartle-Hawking [12], Unruh [13], or Boulware [14]), the Hartle-Hawking state has received the most attention in the literature. This is because the Hartle-Hawking vacuum possesses the most symmetries

(for example, time-reversal symmetry) and so is more straightforward to calculate. Expectation values of observables in this state are also expected to be regular on the event horizon of a black hole. Once the renormalized expectation values in a particular state (say the Hartle-Hawking state) have been computed, it is much easier to compute renormalized expectation values in another state because the difference between expectation values in two states does not require renormalization. A general method for computing $\langle \phi^2 \rangle_{\text{ren}}$ on any static, spherically symmetric, black hole space-time for a state at either a fixed nonzero temperature or zero temperature was developed by Anderson [15], and subsequently extended to calculations of the RSET [1] (see also [16] for an application of this type of approach to the space-time outside a star). This is the method we shall adopt in this paper. This approach works for computations of the Hartle-Hawking (nonzero temperature) and Boulware (zero temperature) states, but not for the Unruh vacuum.

Most of the work on $\langle \phi^2 \rangle_{\text{ren}}$ and the RSET to date has focussed on asymptotically flat black holes, such as Schwarzschild and Reissner-Nordström. However, there are many interesting features of quantum field theory on asymptotically de Sitter black holes [17], when we have both a black hole event horizon and a cosmological horizon. The Kay-Wald theorem [18] states that there is no thermal state on Schwarzschild−de Sitter black holes which preserves all the symmetries of the metric (including time-reversal symmetry) and which is regular on both the event and cosmological horizons. Therefore, there is no equivalent of the Hartle-Hawking state for this geometry. This may be understood heuristically as follows. A thermal state is expected to be regular at a horizon if the temperature of the state matches the temperature of the horizon. However, for Schwarzschild−de Sitter black holes, the temperatures of the event and cosmological horizons are not equal and therefore any thermal state cannot match both temperatures. If we consider the more general case of Reissner-Nordström−de Sitter black holes, then it is possible for the event and cosmological horizons to have the same temperature [19] (these are known as "lukewarm"

*E.Winstanley@sheffield.ac.uk

black holes [20]). Therefore, a natural question is whether the thermal state, constructed on these black holes at the natural temperature, is regular on both the event and cosmological horizons. A simple calculation for two-dimensional black holes [21] shows that this is the case, but for four-dimensional black holes there is an unknown function in the RSET which can only be found by direct calculation. We will return to the computation of this function in the near future [22], but in the present paper we will focus on the simpler computation of $\langle\phi^2\rangle_{\mathrm{ren}}$ for this state.

The outline of this paper is as follows. In Sec. II we review the method of [1] to calculate $\langle\phi^2\rangle_{\mathrm{ren}}$ using point-splitting. As we are considering a thermal quantum state, the Euclidean Green's function will be used. Using temporal point-splitting, even with the points split the Green's function contains apparent divergences. We present in Sec. II B a new approach to regularizing these divergences, based on dimensional reduction. Once the point-split Green's function is manifestly finite, the renormalization procedure is then relatively straightforward, following [1]. The renormalized expectation value $\langle\phi^2\rangle_{\mathrm{ren}}$ is computed numerically for lukewarm black holes in Sec. III. Our numerical results indicate that $\langle\phi^2\rangle_{\mathrm{ren}}$ is indeed regular on both the event and cosmological horizons. This is proved analytically in Sec. IV, in which we use an approximation for the field modes near the horizons, developed in Ref. [23] for the asymptotically flat Reissner-Nordström case. Finally, our conclusions are presented in Sec. V. Throughout this paper the (Lorentzian) metric has signature $(-, +, +, +)$ and we use units in which $8\pi G = \hbar = c = k_B = 1$.

II. GENERAL METHOD TO CALCULATE $\langle\phi^2\rangle_{\mathrm{ren}}$

A. Point-split Green's function

We use the method of Refs. [1,15] to compute the renormalized expectation value $\langle\phi^2\rangle_{\mathrm{ren}}$. In this section we just briefly outline the key steps in the construction, further details of which can be found in Refs. [1,15].

We begin with a scalar field ϕ with mass m and coupling ξ to the scalar curvature R, satisfying the field equation

$$(\nabla_\mu\nabla^\mu - m^2 - \xi R)\phi = 0. \qquad (2.1)$$

In this paper we consider a black hole space-time with metric, in Schwarzschild-like coordinates, given by

$$ds^2 = -f(r)dt^2 + f(r)^{-1}dr^2 + r^2 d\theta^2 + r^2\sin^2\theta d\varphi^2, \qquad (2.2)$$

where the metric function f depends only on the radial coordinate r. The metric (2.2) is not the most general spherically symmetric black hole metric, and, indeed, the method of Ref. [1] is developed for more general spherically symmetric metrics. However, the metric (2.2) is sufficiently general to cover a broad class of black hole

geometries, including, in particular, the Reissner-Nordström–de Sitter black holes for which

$$f(r) = 1 - \frac{2M}{r} + \frac{Q^2}{r^2} - \frac{\Lambda r^2}{3}, \qquad (2.3)$$

where M, Q are related, respectively, to the mass and charge of the black hole [24] and Λ is the (positive) cosmological constant. Further details of the space-time geometry in which we are particularly interested, the lukewarm black holes, will be given in Sec. III A.

We are interested in computing $\langle\phi^2\rangle_{\mathrm{ren}}$ for a thermal state at a temperature T. We follow [1] and use a Euclidean space approach. By defining the Euclidean time τ as $\tau = it$, the metric (2.2) becomes

$$ds^2 = f(r)d\tau^2 + f(r)^{-1}dr^2 + r^2 d\theta^2 + r^2\sin^2\theta d\varphi^2. \qquad (2.4)$$

We define $G_E(x; x')$ to be the Euclidean Green's function, which satisfies the equation [1]

$$[\nabla_{x\mu}\nabla_x^\mu - m^2 - \xi R]G_E(x; x') = -g^{-(1/2)}(x)\delta^4(x, x'), \qquad (2.5)$$

where the covariant derivative is now taken with respect to the metric (2.4). Using the method of point-splitting, the (unrenormalized) expectation value $\langle\phi^2\rangle_{\mathrm{unren}}$ is given by the following limit:

$$\langle\phi^2\rangle_{\mathrm{unren}} = \Re[\lim_{x\to x'} G_E(x; x')]. \qquad (2.6)$$

The stress-energy tensor is calculated from derivatives of $G_E(x; x')$ [1].

For a thermal state at a temperature T, the Euclidean Green's function $G_E(x; x')$ is periodic in $\tau - \tau'$ with period T^{-1}. In this case the scalar Euclidean Green's function takes the form [1,15]

$$G_E(x; x') = \frac{T}{4\pi}\sum_{n=-\infty}^{\infty}\exp[i\omega(\tau - \tau')]$$
$$\times \sum_{\ell=0}^{\infty}(2\ell + 1)P_\ell(\cos\gamma)\mathrm{Y}_{\omega\ell}(r, r'), \qquad (2.7)$$

where $\omega = 2\pi nT$, and P_ℓ is the usual Legendre function, with

$$\cos\gamma = \cos\theta\cos\theta' + \sin\theta\sin\theta'\cos(\varphi - \varphi'), \qquad (2.8)$$

and $\mathrm{Y}_{\omega\ell}$ satisfies the differential equation

$$-\frac{1}{r^2}\delta(r - r') = f\frac{d^2\mathrm{Y}_{\omega\ell}}{dr^2} + \left(\frac{2f}{r} + \frac{df}{dr}\right)\frac{d\mathrm{Y}_{\omega\ell}}{dr}$$
$$- \left[\frac{\omega^2}{f} + \frac{\ell(\ell + 1)}{r^2} + m^2 + \xi R\right]\mathrm{Y}_{\omega\ell}. \qquad (2.9)$$

The differential equation (2.9) arises from separating the wave Eq. (2.5) on the background metric (2.4).

We define functions $p_{\omega\ell}$ and $q_{\omega\ell}$ as solutions of the corresponding homogeneous differential equation

$$0 = f\frac{d^2 \Upsilon_{\omega\ell}}{dr^2} + \left(\frac{2f}{r} + \frac{df}{dr}\right)\frac{d\Upsilon_{\omega\ell}}{dr}$$
$$- \left[\frac{\omega^2}{f} + \frac{\ell(\ell+1)}{r^2} + m^2 + \xi R\right]\Upsilon_{\omega\ell}, \qquad (2.10)$$

with appropriate boundary conditions. These will be discussed further in Sec. III B for the particular case of lukewarm black holes. Typically, $p_{\omega\ell}$ is the solution which is regular at the lower limit of the region under consideration (for black holes, the event horizon), while $q_{\omega\ell}$ is regular at the upper limit of the region (usually infinity, but in our case the cosmological horizon). The function $\Upsilon_{\omega\ell}(r, r')$ is then given by [15]

$$\Upsilon_{\omega\ell}(r, r') = C_{\omega\ell}\, p_{\omega\ell}(r_<)\, q_{\omega\ell}(r_>), \qquad (2.11)$$

where, as usual, $r_<$ is the lesser of the two values r, r' and $r_>$ is the greater. In (2.11), the normalization constant $C_{\omega\ell}$ is fixed by the normalization condition [15]

$$C_{\omega\ell}\left[p_{\omega\ell}\frac{dq_{\omega\ell}}{dr} - q_{\omega\ell}\frac{dp_{\omega\ell}}{dr}\right] = -\frac{1}{r^2 f}. \qquad (2.12)$$

Further properties of the mode functions $p_{\omega\ell}$ and $q_{\omega\ell}$ will be discussed in Sec. III B.

We now follow standard procedure and choose temporal point-splitting, so that $r = r'$, $\theta = \theta'$, and $\varphi = \varphi'$. Then $\gamma = 1$ (2.8) and, using $P_\ell(1) = 1$, we have

$$G_E(\tau, \boldsymbol{x}; \tau', \boldsymbol{x}) = \frac{T}{4\pi}\sum_{n=-\infty}^{\infty}e^{i\omega\epsilon}\sum_{\ell=0}^{\infty}(2\ell+1)$$
$$\times C_{\omega\ell}\, p_{\omega\ell}(r)\, q_{\omega\ell}(r), \qquad (2.13)$$

where $\epsilon = \tau - \tau'$.

B. Finite mode sums

Even though the points are separated, the Green's function (2.13) is apparently divergent. This is due to our choice of point-splitting and arises in practice because the sums over ℓ in (2.13) do not converge. This problem is well known, arising first in Candelas's [5] calculations on a Schwarzschild background. This divergence cannot be "real" since, by definition, the Green's function *must* be finite when the points are separated. The apparent divergences are removed by subtracting from (2.13) a suitable multiple of the delta function (which vanishes when the points are separated). The answer is well known, and given by [1,15]:

$$G_E(\tau, \boldsymbol{x}; \tau', \boldsymbol{x}) = \frac{T}{4\pi}\sum_{n=-\infty}^{\infty}e^{i\omega\epsilon}\sum_{\ell=0}^{\infty}\Bigg[(2\ell+1)$$
$$\times C_{\omega\ell}\, p_{\omega\ell}(r)\, q_{\omega\ell}(r) - \frac{1}{rf^{(1/2)}}\Bigg]. \qquad (2.14)$$

Although this answer has been previously calculated, in this section we would like to take a different approach to deriving the result (2.14) based on dimensional reduction. This new method may prove to be useful in more complicated situations (such as Kerr black holes).

We begin by writing the general Euclidean Green's function (2.7) in the form

$$G_E(x; x') = \frac{T}{4\pi}\sum_{n=-\infty}^{\infty}\exp[i\omega(\tau - \tau')]$$
$$\times \mathcal{G}_\omega(r, \theta, \varphi; r', \theta', \varphi'), \qquad (2.15)$$

where

$$\mathcal{G}_\omega(r, \theta, \varphi; r', \theta', \varphi') = \sum_{\ell=0}^{\infty}(2\ell+1)\Upsilon_{\omega\ell}(r, r')P_\ell(\cos\gamma). \qquad (2.16)$$

Using the wave equation (2.5), the function $\mathcal{G}_\omega(r, \theta, \varphi; r', \theta', \varphi')$ satisfies the differential equation

$$-\frac{\delta(\boldsymbol{x}, \boldsymbol{x}')}{r^2 \sin\theta} = \frac{1}{r^2}\frac{\partial}{\partial r}\left[fr^2\frac{\partial \mathcal{G}_\omega}{\partial r}\right] + \frac{1}{r^2 \sin\theta}\frac{\partial}{\partial \theta}\left[\sin\theta\frac{\partial \mathcal{G}_\omega}{\partial \theta}\right]$$
$$+ \frac{1}{r^2 \sin^2\theta}\frac{\partial^2 \mathcal{G}_\omega}{\partial \varphi^2} - \left[\frac{\omega^2}{f} + m^2 + \xi R\right]\mathcal{G}_\omega. \qquad (2.17)$$

Equation (2.17) looks very much like a wave equation in three dimensions, with a potential term:

$$\tilde{V} = \frac{\omega^2}{f} + m^2 + \xi R. \qquad (2.18)$$

In fact, by multiplying (2.17) by f^{-1}, we obtain the wave equation on the three-metric

$$d\tilde{s}^2 = dr^2 + r^2 f d\theta^2 + r^2 f \sin^2\theta d\varphi^2, \qquad (2.19)$$

namely,

$$[\tilde{\nabla}_i\tilde{\nabla}^i - V(\boldsymbol{x})]\mathcal{G}_\omega(\boldsymbol{x}; \boldsymbol{x}') = -\tilde{g}^{-(1/2)}(\boldsymbol{x})\delta^3(\boldsymbol{x}, \boldsymbol{x}'), \qquad (2.20)$$

where the covariant derivatives are with respect to the three-metric (2.19) (acting on $\boldsymbol{x}$) and $\tilde{g}$ is the determinant of the three-metric (2.19), with the potential

$$V(\boldsymbol{x}) = \frac{\tilde{V}}{f} = \frac{\omega}{f^2} + \frac{m^2 + \xi R}{f}, \qquad (2.21)$$

where it should be stressed that R is the Ricci scalar of the *original*, four-dimensional, metric (2.4).

The three-metric (2.19) is curious. We emphasize that it has no physical significance, and in fact it has a curvature singularity at an event horizon where f vanishes. Furthermore, the potential (2.21) is also divergent at a horizon. On the other hand, if we are dealing with an asymptotically flat metric (2.2), then the three-metric (2.19) is also asymptotically flat as $f \to 1$ at infinity. The

three-metric should simply be regarded as a useful mathematical tool.

From Eq. (2.20), we can see that $\mathcal{G}_\omega(\boldsymbol{x}; \boldsymbol{x}')$ is indeed a three-dimensional Euclidean Green's function for a scalar field on the three-metric (2.19), but with an unusual potential (2.21). However, the potential does not affect the general form of the singularity structure of the Green's function, which has the usual Hadamard form in three dimensions [25,26]:

$$\mathcal{G}_\omega(\boldsymbol{x}, \boldsymbol{x}') = \frac{U(\boldsymbol{x}, \boldsymbol{x}')}{[2\sigma(\boldsymbol{x}, \boldsymbol{x}')]^{(1/2)}} + W(\boldsymbol{x}, \boldsymbol{x}'). \qquad (2.22)$$

Here, $2\sigma(\boldsymbol{x}, \boldsymbol{x}')$ is the square of the geodesic distance between two closely separated points $\boldsymbol{x}$, $\boldsymbol{x}'$, and $U(\boldsymbol{x}, \boldsymbol{x}')$, $W(\boldsymbol{x}, \boldsymbol{x}')$ are symmetric biscalars which are regular in the limit $\boldsymbol{x} \to \boldsymbol{x}'$, whose precise form will depend on the potential $V(\boldsymbol{x})$. Note that there is no logarithmic term in the Hadamard expansion (2.22) as we are currently working in three rather than four dimensions. The biscalars $U(\boldsymbol{x}, \boldsymbol{x}')$ and $W(\boldsymbol{x}, \boldsymbol{x}')$ can be expanded in terms of $\sigma(\boldsymbol{x}, \boldsymbol{x}')$ using standard methods [26,27]. For our purposes here, we only require the lowest order term in $U(\boldsymbol{x}, \boldsymbol{x}')$:

$$U(\boldsymbol{x}, \boldsymbol{x}') = 1 + O(\sigma), \qquad (2.23)$$

which does not depend on the potential V (2.21).

We now choose a point-splitting for the three-dimensional Green's function $\mathcal{G}_\omega$. We choose $r = r'$ and $\varphi = \varphi'$. Since the metric (2.19) is spherically symmetric, we can, without loss of generality, fix $\theta' = 0$, and then $\cos\gamma = \cos\theta$ (2.8) and (2.16) takes the form

$$\mathcal{G}_\omega(r, \theta, \varphi; r, 0, \varphi) = \sum_{\ell=0}^{\infty} (2\ell + 1)$$
$$\times C_{\omega\ell} p_{\omega\ell}(r) q_{\omega\ell}(r) P_\ell(\cos\theta). \quad (2.24)$$

Although we have brought the radial coordinates together, this sum is still finite because of the $P_\ell(\cos\theta)$ terms. For this point-splitting, to leading order we have

$$2\sigma = r^2 f \theta^2 + O(\theta^4). \qquad (2.25)$$

Therefore the Hadamard form (2.22) reads

$$\mathcal{G}_\omega(r, \theta, \varphi; r, 0, \varphi) = \frac{1}{r f^{(1/2)} \theta} + \text{finite terms}, \quad (2.26)$$

so that, for small θ, we have

$$\sum_{\ell=0}^{\infty} (2\ell + 1) C_{\omega\ell} p_{\omega\ell}(r) q_{\omega\ell}(r) P_\ell(\cos\theta) = \frac{1}{r f^{(1/2)} \theta} + O(1). \qquad (2.27)$$

This clearly shows that the sums over ℓ in (2.13) diverge.

We find the appropriate subtraction term to render the sums over ℓ finite using the identity [3]

$$\sum_{\ell=0}^{\infty} P_\ell(\cos\theta) = \frac{1}{\theta} + O(\theta). \qquad (2.28)$$

Multiplying this by $1/(r f^{1/2})$ and subtracting, we therefore obtain

$$\sum_{\ell=0}^{\infty} \left[(2\ell + 1) C_{\omega\ell} p_{\omega\ell}(r) q_{\omega\ell}(r) - \frac{1}{r f^{(1/2)}} \right] P_\ell(\cos\theta) = O(1). \qquad (2.29)$$

We may now take the limit $\theta \to 0$ and find that the sums over ℓ in (2.14) are finite as required.

C. Renormalized expectation value

From (2.14), we now have an expression for the unrenormalized expectation value $\langle \phi^2 \rangle_{\text{unren}}$:

$$\langle \phi^2 \rangle_{\text{unren}} = \lim_{\epsilon \to 0} \left\{ \frac{T}{4\pi} \sum_{n=-\infty}^{\infty} \cos(\omega\epsilon) \sum_{\ell=0}^{\infty} \left[(2\ell + 1) \right. \right.$$
$$\left. \times C_{\omega\ell} p_{\omega\ell}(r) q_{\omega\ell}(r) - \frac{1}{r f^{(1/2)}} \right] \right\}$$
$$= \lim_{\epsilon \to 0} \left\{ \frac{T}{2\pi} \sum_{n=1}^{\infty} \cos(\omega\epsilon) \sum_{\ell=0}^{\infty} \left[(2\ell + 1) \right. \right.$$
$$\left. \times C_{\omega\ell} p_{\omega\ell}(r) q_{\omega\ell}(r) - \frac{1}{r f^{(1/2)}} \right]$$
$$+ \frac{T}{4\pi} \sum_{\ell=0}^{\infty} \left[(2\ell + 1) C_{0\ell} p_{0\ell}(r) q_{0\ell}(r) - \frac{1}{r f^{(1/2)}} \right] \right\}. \qquad (2.30)$$

To renormalize this expression, we subtract the usual divergent terms $\langle \phi^2 \rangle_{\text{div}}$ before taking the limit $\epsilon \to 0$ [28]:

$$\langle \phi^2 \rangle_{\text{div}} = \frac{1}{8\pi^2 \sigma} + \frac{1}{8\pi^2} \left[m^2 + \left(\xi - \frac{1}{6} \right) R \right]$$
$$\times \left[C + \frac{1}{2} \ln\left(\frac{\mu^2 |\sigma|}{2} \right) \right] - \frac{m^2}{16\pi^2}$$
$$+ \frac{1}{96\pi^2} R_{\alpha\beta} \frac{\sigma^\alpha \sigma^\beta}{\sigma}, \qquad (2.31)$$

where $\sigma^\alpha = \sigma^{;\alpha}$, the quantity C is Euler's constant, and $R_{\alpha\beta}$ is the (four-dimensional) Ricci tensor. If we are considering a massive scalar field, then the constant μ is simply equal to m, the mass of the field. However, for a massless scalar field, the constant μ is arbitrary [1]. It corresponds in the massless case to a finite renormalization of terms in the gravitational action.

For our particular point-splitting, the quantities appearing in (2.31) have already been computed [1,15,28]:

$$\sigma = \frac{1}{2}f\epsilon^2 - \frac{1}{96}f\left(\frac{df}{dr}\right)^2\epsilon^4 + O(\epsilon^6);$$

$$\sigma^\tau = -\epsilon + \frac{1}{24}\left(\frac{df}{dr}\right)^2\epsilon^3 + O(\epsilon^5);$$

$$\sigma^r = \frac{1}{4}f\frac{df}{dr}\epsilon^2 + O(\epsilon^4); \qquad (2.32)$$

$$\sigma^\theta = \sigma^\varphi = 0.$$

The subtraction terms (2.31) then simplify to [15]:

$$\langle\phi^2\rangle_{\mathrm{div}} = \frac{1}{4\pi^2\epsilon^2 f} + \frac{1}{8\pi^2}\left[m^2 + \left(\xi - \frac{1}{6}\right)R\right]$$

$$\times\left[C + \frac{1}{2}\ln\left(\frac{\mu^2 f\epsilon^2}{4}\right)\right] - \frac{m^2}{16\pi^2} + \frac{1}{192\pi^2 f}\left(\frac{df}{dr}\right)^2$$

$$- \frac{1}{96\pi^2}\frac{d^2f}{dr^2} - \frac{1}{48\pi^2 r}\frac{df}{dr}. \qquad (2.33)$$

In order to subtract (2.33) from (2.30), we first need to write (2.33) in terms of mode sums. This is done using the following identities, valid for small ϵ and any $\kappa > 0$ [1,3]:

$$\frac{1}{\epsilon^2} = -\kappa^2\sum_{n=1}^\infty n\cos(n\kappa\epsilon) - \frac{\kappa^2}{12} + O(\epsilon^2);$$

$$-\frac{1}{2}\ln(\kappa^2\epsilon^2) = \sum_{n=1}^\infty\frac{\cos(n\kappa\epsilon)}{n} + O(\epsilon^2). \qquad (2.34)$$

We choose $\kappa = 2\pi T$, so that ω in Eq. (2.30) is equal to $n\kappa$. Then the subtraction terms (2.33) become

$$\langle\phi^2\rangle_{\mathrm{div}} = -\frac{\kappa}{4\pi^2 f}\sum_{n=1}^\infty\omega\cos(\omega\epsilon) - \frac{\kappa}{8\pi^2}\left[m^2 + \left(\xi - \frac{1}{6}\right)R\right]$$

$$\times\sum_{n=1}^\infty\frac{\cos(\omega\epsilon)}{\omega} + \frac{1}{8\pi^2}\left[m^2 + \left(\xi - \frac{1}{6}\right)R\right]$$

$$\times\left[C + \frac{1}{2}\ln\left(\frac{\mu^2 f}{4\kappa^2}\right)\right] - \frac{m^2}{16\pi^2} + \frac{1}{192\pi^2 f}\left(\frac{df}{dr}\right)^2$$

$$- \frac{1}{96\pi^2}\frac{d^2f}{dr^2} - \frac{1}{48\pi^2 r}\frac{df}{dr} - \frac{\kappa^2}{48\pi^2 f} + O(\epsilon^2). \qquad (2.35)$$

This is now in a form suitable for subtracting from (2.30), and the limit $\epsilon \to 0$ can then be taken to give the final, renormalized, expectation value [1]:

$$\langle\phi^2\rangle_{\mathrm{ren}} = \langle\phi^2\rangle_{\mathrm{analytic}} + \langle\phi^2\rangle_{\mathrm{numeric}} \qquad (2.36)$$

where

$$\langle\phi^2\rangle_{\mathrm{analytic}} = \frac{m^2}{16\pi^2} - \frac{1}{192\pi^2 f}\left(\frac{df}{dr}\right)^2 + \frac{1}{96\pi^2}\frac{d^2f}{dr^2}$$

$$+ \frac{1}{48\pi^2 r}\frac{df}{dr} + \frac{\kappa^2}{48\pi^2 f} - \frac{1}{8\pi^2}\left[m^2 + \left(\xi - \frac{1}{6}\right)R\right]$$

$$\times\left[C + \frac{1}{2}\ln\left(\frac{\mu^2 f}{4\kappa^2}\right)\right]; \qquad (2.37)$$

$$\langle\phi^2\rangle_{\mathrm{numeric}} = \frac{T}{2\pi}\sum_{n=1}^\infty\left\{\sum_{\ell=0}^\infty\left[(2\ell+1)C_{\omega\ell}p_{\omega\ell}(r)q_{\omega\ell}(r) - \frac{1}{r\sqrt{f}}\right]\right.$$

$$+ \frac{\omega}{f} + \frac{1}{2\omega}\left[m^2 + \left(\xi - \frac{1}{6}\right)R\right]\right\}$$

$$+ \frac{T}{4\pi}\sum_{\ell=0}^\infty\left[(2\ell+1)C_{0\ell}p_{0\ell}(r)q_{0\ell}(r) - \frac{1}{r\sqrt{f}}\right].$$

$$(2.38)$$

As the name suggests, $\langle\phi^2\rangle_{\mathrm{analytic}}$ has a simple form which can be easily computed for any κ and metric function f. On the other hand, the quantity $\langle\phi^2\rangle_{\mathrm{numeric}}$ can, in general, only be computed numerically as the mode equation (2.10) needs to be integrated. Solutions to the mode equation are not known in closed form for general ω even for Schwarzschild black holes. One might hope that $\langle\phi^2\rangle_{\mathrm{analytic}}$ is a good approximation to $\langle\phi^2\rangle_{\mathrm{ren}}$, at least in some region of the space-time. This is discussed in [1] for the case of Reissner-Nordström black holes, and we will examine this issue for lukewarm black holes in Sec. III.

D. Computation of $\langle\phi^2\rangle_{\mathrm{numeric}}$

Before we can compute $\langle\phi^2\rangle_{\mathrm{numeric}}$, further work is needed. The mode sums in $\langle\phi^2\rangle_{\mathrm{numeric}}$ converge so slowly as to render their numerical computation impractical. We therefore employ a WKB-like approximation, which will give the large ω, ℓ behavior of the mode sums in (2.38). We have found it simplest to use the WKB approach of Howard [3], which is different from that used in Refs. [1,15].

Define a new function $\beta_{\omega\ell}(r)$ for $\omega \neq 0$ by

$$\beta_{\omega\ell}(r) = C_{\omega\ell}p_{\omega\ell}(r)q_{\omega\ell}(r). \qquad (2.39)$$

Then $\beta_{\omega\ell}$ satisfies the following differential equation (cf. [3]):

$$\beta_{\omega\ell} = \frac{1}{2\chi_{\omega\ell}}\left[1 - \frac{1}{\chi_{\omega\ell}^2}\left(\frac{1}{\sqrt{\beta_{\omega\ell}}}\frac{d^2(\sqrt{\beta_{\omega\ell}})}{d\zeta^2} - \eta\right)\right]^{-(1/2)},$$

$$(2.40)$$

where we have defined a new independent variable ζ by

$$\frac{d}{d\zeta} = r^2 f\frac{d}{dr}, \qquad (2.41)$$

and the functions $\chi_{\omega\ell}(r)$ and $\eta(r)$ are given by

$$\chi_{\omega\ell}(r) = \sqrt{\omega^2 r^4 + \left(\ell + \frac{1}{2}\right)^2 r^2 f},$$

$$\eta(r) = -\frac{1}{4}fr^2 + (m^2 + \xi R)fr^4. \tag{2.42}$$

We are looking for the behavior of $\beta_{\omega\ell}(r)$ when either ω or ℓ are large, that is, when $\chi_{\omega\ell}(r)$ is large. This is found by inserting a fictitious parameter ε into (2.40) as follows:

$$\beta_{\omega\ell} = \frac{1}{2\chi_{\omega\ell}}\left[1 - \frac{1}{\varepsilon^2\chi_{\omega\ell}^2}\left(\frac{1}{\sqrt{\beta_{\omega\ell}}}\frac{d^2(\sqrt{\beta_{\omega\ell}})}{d\zeta^2} - \eta\right)\right], \tag{2.43}$$

and then expanding $\beta_{\omega\ell}$ in inverse powers of ε:

$$\beta_{\omega\ell}(r) = \beta_{0\omega\ell}(r) + \varepsilon^{-2}\beta_{1\omega\ell}(r) + \varepsilon^{-4}\beta_{2\omega\ell}(r) + \dots, \tag{2.44}$$

finally setting $\varepsilon = 1$ at the end of the calculation.

It is straightforward to read off from (2.43) that $\beta_{0\omega\ell}(r)$ has the simple form

$$\beta_{0\omega\ell}(r) = \frac{1}{2\chi_{\omega\ell}(r)}. \tag{2.45}$$

The next term in the expansion $\beta_{1\omega\ell}(r)$ is more complicated but not difficult to calculate:

$$\beta_{1\omega\ell}(r) = -\frac{r^6 f}{64\chi_{\omega\ell}^7}(A_1\chi_{\omega\ell}^4 + B_1\chi_{\omega\ell}^2 + C_1), \tag{2.46}$$

where

$$A_1 = \frac{1}{f^2 r^4}\left[-fr^2\left(\frac{df}{dr}\right)^2 + 12f^2 r\frac{df}{dr} + 4f^3 - 4f^2\right.$$
$$\left. + 16r^2\xi Rf^2 + 4f^2 r^2\frac{d^2 f}{dr^2} + 16r^2 m^2 f^2\right];$$

$$B_1 = \frac{\omega^2}{f^2}\left[-4f^2 r^2\frac{d^2 f}{dr^2} + 6fr^2\left(\frac{df}{dr}\right)^2\right.$$
$$\left. - 16f^2 r\frac{df}{dr} + 16f^3\right];$$

$$C_1 = -5\frac{\omega^4 r^4}{f}\left[4f^2 + r^2\left(\frac{df}{dr}\right)^2 - 4fr\frac{df}{dr}\right]. \tag{2.47}$$

It can be seen from (2.45) and (2.46) that, for large $\chi_{\omega\ell}$ (or, equivalently, for large ω or ℓ if $f \neq 0$),

$$\beta_{0\omega\ell} \sim \chi_{\omega\ell}^{-1}, \qquad \beta_{1\omega\ell} \sim \chi_{\omega\ell}^{-3}, \tag{2.48}$$

and we find similarly that $\beta_{2\omega\ell} \sim \chi_{\omega\ell}^{-5}$ etc. If we consider the sum

$$\sum_{n=1}^{\infty}\sum_{\ell=0}^{\infty}(2\ell + 1)[C_{\omega\ell}p_{\omega\ell}(r)q_{\omega\ell}(r) - \beta_{0\omega\ell}(r) - \beta_{1\omega\ell}(r)], \tag{2.49}$$

then the summand is $O(\ell^{-4})$ for large ℓ. This is the behavior we observe when we compute the summand

numerically in Sec. III B. When this is summed over ℓ, we obtain a summand which is $O(\omega^{-3})$ and therefore converges rapidly. Therefore it is sufficient to subtract just $\beta_{0\omega\ell}$ and $\beta_{1\omega\ell}$ from the mode sums in $\langle\phi^2\rangle_{\text{numeric}}$ (2.38).

The contribution to (2.38) from the $\omega = 0$ modes needs to be considered separately. When $\omega = 0$, from (2.42) we have $\chi_{0\ell} = (\ell + \frac{1}{2})rf^{(1/2)}$ and therefore (2.45) and (2.46) become

$$\beta_{00\ell}(r) = \frac{1}{2rf^{(1/2)}}\left(\ell + \frac{1}{2}\right)^{-1};$$

$$\beta_{10\ell}(r) = -\frac{r^3}{64f^{(1/2)}}A_1\left(\ell + \frac{1}{2}\right)^{-3}. \tag{2.50}$$

Therefore $(2\ell + 1)\beta_{00\ell}(r) = (rf^{(1/2)})^{-1}$ and this part of the WKB approximation has already been subtracted from the sum. In this case we consider

$$\sum_{\ell=0}^{\infty}(2\ell + 1)[C_{0\ell}p_{0\ell}(r)q_{0\ell}(r) - \beta_{00\ell}(r) - \beta_{10\ell}(r)], \tag{2.51}$$

and again the summand is $O(\ell^{-4})$ for large ℓ as required.

We therefore write

$$\langle\phi^2\rangle_{\text{numeric}} = \frac{T}{2\pi}\sum_{n=1}^{\infty}\left\{\sum_{\ell=0}^{\infty}(2\ell + 1)[C_{\omega\ell}p_{\omega\ell}(r)q_{\omega\ell}(r)\right.$$
$$- \beta_{0\omega\ell}(r) - \beta_{1\omega\ell}(r)]$$
$$+ \sum_{\ell=0}^{\infty}\left[(2\ell + 1)[\beta_{0\omega\ell}(r) + \beta_{1\omega\ell}(r)] - \frac{1}{rf^{(1/2)}}\right]$$
$$+ \frac{\omega}{f} + \frac{1}{2\omega}\left[m^2 + \left(\xi - \frac{1}{6}\right)R\right]\right\}$$
$$+ \frac{T}{4\pi}\left\{\sum_{\ell=0}^{\infty}(2\ell + 1)[C_{0\ell}p_{0\ell}(r)q_{0\ell}(r) - \beta_{00\ell}(r)\right.$$
$$\left. - \beta_{10\ell}(r)] + \sum_{\ell=0}^{\infty}(2\ell + 1)\beta_{10\ell}(r)\right\}, \tag{2.52}$$

where we have used the fact that $(2\ell + 1)\beta_{00\ell}(r) = (rf^{(1/2)})^{-1}$. The sums in the first two lines and last two lines of (2.52) are now amenable to numerical computation. The final sum is readily computed using (2.50) to be

$$\sum_{\ell=0}^{\infty}(2\ell + 1)\beta_{10\ell}(r) = -\frac{r^3}{64f^{(1/2)}}A_1\sum_{\ell=0}^{\infty}2\left(\ell + \frac{1}{2}\right)^{-2}$$
$$= -\frac{\pi^2 r^3}{64f^{(1/2)}}A_1. \tag{2.53}$$

Since we have analytic expressions for $\beta_{0\omega\ell}(r)$ and $\beta_{1\omega\ell}(r)$, we next examine the term

$$\sum_{n=1}^{\infty}\left\{\sum_{\ell=0}^{\infty}(2\ell+1)\left[\left(\beta_{0\omega\ell(r)}-\frac{1}{rf^{(1/2)}}\right)+\beta_{1\omega\ell}(r)\right]\right.$$
$$\left.+\frac{\omega}{f}+\frac{1}{2\omega}\left[m^2+\left(\xi-\frac{1}{6}\right)R\right]\right\}. \quad (2.54)$$

The sums over ℓ are most easily found using the Watson-Sommerfeld formula (see, for example, [4]), valid for any function analytic in the right-hand half plane:

$$\sum_{\ell=0}^{\infty}\mathcal{F}(\ell)=\int_0^{\infty}\mathcal{F}\left(\lambda-\frac{1}{2}\right)d\lambda$$
$$-\Re\left[i\int_0^{\infty}\frac{2}{1+e^{2\pi\lambda}}\mathcal{F}\left(i\lambda-\frac{1}{2}\right)d\lambda\right]. \quad (2.55)$$

Using (2.55), we write, for $\omega\neq0$,

$$\sum_{\ell=0}^{\infty}(2\ell+1)\left[\beta_{0\omega\ell(r)}-\frac{1}{rf^{(1/2)}}\right]=I_0(\omega,r)+\tilde{J}_0(\omega,r);$$
$$\sum_{\ell=0}^{\infty}(2\ell+1)\beta_{1\omega\ell(r)}=I_1(\omega,r)+J_1(\omega,r);$$
$$(2.56)$$

where the $I_i(\omega,r)$ are the integrals from the first term in (2.55) and the $J_i(\omega,r)$ are the integrals from the second term in (2.55). The $I_i(\omega,r)$ integrals are easily calculated for $\omega\neq0$ (here $\ell=\lambda-1/2$):

$$I_0(\omega,r)=\int_0^{\infty}\left[2\lambda\beta_{0\omega\ell}(r)-\frac{1}{rf^{(1/2)}}\right]d\lambda=-\frac{\omega}{f};$$
$$I_1(\omega,r)=\int_0^{\infty}2\lambda\beta_{1\omega\ell}(r)d\lambda \quad (2.57)$$
$$=-\frac{1}{2\omega}\left[m^2+\left(\xi-\frac{1}{6}\right)R\right]-\frac{1}{24r^2\omega}.$$

Substituting these results in (2.52) gives

$$\langle\phi^2\rangle_{\text{numeric}}=\frac{T}{2\pi}\sum_{n=1}^{\infty}\left\{\sum_{\ell=0}^{\infty}(2\ell+1)[C_{\omega\ell}p_{\omega\ell}(r)q_{\omega\ell}(r)\right.$$
$$-\beta_{0\omega\ell}(r)-\beta_{1\omega\ell}(r)]+\tilde{J}_0(\omega,r)+J_1(\omega,r)$$
$$\left.-\frac{1}{24r^2\omega}\right\}+\frac{T}{4\pi}\left\{\sum_{\ell=0}^{\infty}(2\ell+1)[C_{0\ell}p_{0\ell}(r)q_{0\ell}(r)\right.$$
$$\left.-\beta_{00\ell}(r)-\beta_{10\ell}(r)]-\frac{\pi^2r^3}{64f^{(1/2)}}A_1\right\}. \quad (2.58)$$

Next we examine the $J_i(\omega,r)$ integrals (here $\ell=i\lambda-1/2$):

$$\tilde{J}_0(\omega,r)=-\Re\left\{i\int_0^{\infty}\frac{2}{1+e^{2\pi\lambda}}\left[2\lambda i\beta_{0\omega\ell}(r)\right.\right.$$
$$\left.\left.-\frac{1}{rf^{(1/2)}}\right]d\lambda\right\}, \quad (2.59)$$
$$J_1(\omega,r)=\Re\left\{\int_0^{\infty}\frac{4\lambda}{1+e^{2\pi\lambda}}\beta_{1\omega\ell}(r)d\lambda\right\}.$$

We consider each of these in turn. First, for $\tilde{J}_0(\omega,r)$, substituting in the form of $\beta_{0\omega\ell}(r)$ (2.45) gives

$$\tilde{J}_0(\omega,r)=\frac{1}{rf^{(1/2)}}\Re\left[\int_0^{\infty}\frac{2i}{1+e^{2\pi\lambda}}d\lambda\right.$$
$$+\int_0^a\frac{2\lambda}{(1+e^{2\pi\lambda})(a^2-\lambda^2)^{(1/2)}}d\lambda$$
$$\left.+\int_a^{\infty}\frac{2\lambda}{(1+e^{2\pi\lambda})(a^2-\lambda^2)^{(1/2)}}d\lambda\right], \quad (2.60)$$

where we have defined

$$a=\frac{\omega r}{f^{(1/2)}}. \quad (2.61)$$

The first and third integrals in (2.60) do not contribute, leaving just the second integral. The integrand is integrable but not regular at $\lambda=a$. Furthermore, this integral is not known in closed form and will need to be computed numerically. It is easier numerically to have a regular integrand, so we integrate once by parts to obtain

$$\tilde{J}_0(\omega,r)=\frac{\omega}{f}-\frac{4\pi\omega}{f}\int_0^a\left(1-\frac{\lambda^2}{a^2}\right)^{(1/2)}\frac{e^{2\pi\lambda}}{(1+e^{2\pi\lambda})^2}d\lambda. \quad (2.62)$$

For large ω, this integral behaves like

$$\tilde{J}_0(\omega,r)=\frac{1}{24\omega r^2}+O(\omega^{-3}). \quad (2.63)$$

We therefore take the $-(24\omega r^2)^{-1}$ term from (2.58) and consider instead

$$J_0(\omega,r)=\frac{\omega}{f}-\frac{1}{24r^2\omega}-\frac{4\pi\omega}{f}\int_0^a\left(1-\frac{\lambda^2}{a^2}\right)^{(1/2)}$$
$$\times\frac{e^{2\pi\lambda}}{(1+e^{2\pi\lambda})^2}d\lambda\sim O(\omega^{-3}) \quad (2.64)$$

as $\omega\to\infty$. This means that the sum $\sum_{n=1}^{\infty}J_0(\omega,r)$ can be computed separately from the other terms in $\langle\phi^2\rangle_{\text{numeric}}$ (2.58).

The integral $J_1(\omega,r)$ is more complicated. Using the form (2.46) of $\beta_{1\omega\ell}(r)$, we find

$$J_1(\omega,r)=-\frac{1}{16rf^{(1/2)}}\left[r^4A_1K_1(\omega,r)+\frac{1}{\omega^2}B_2K_2(\omega,r)\right.$$
$$\left.+\frac{1}{\omega^4r^4}C_1K_3(\omega,r),\right] \quad (2.65)$$

where we have defined new integrals

$$K_1(\omega, r) = \frac{1}{a}\Re\left[\int_0^\infty \frac{q}{(1-q^2)^{(3/2)}(1+e^{2\pi aq})}\,dq\right];$$

$$K_2(\omega, r) = \frac{1}{a}\Re\left[\int_0^\infty \frac{q}{(1-q^2)^{(5/2)}(1+e^{2\pi aq})}\,dq\right];$$

$$K_3(\omega, r) = \frac{1}{a}\Re\left[\int_0^\infty \frac{q}{(1-q^2)^{(7/2)}(1+e^{2\pi aq})}\,dq\right];$$

$$(2.66)$$

and $q = \lambda/a$. The integrands in all three integrals have branch points at $q = \pm 1$, so we cut the plane along the interval $[-1, 1]$ and consider the contour shown in Fig. 1. The contribution to each $K_i(\omega, r)$ from the contour γ_2 is zero, so we write, for each $i = 1, 2, 3$:

$$K_i(\omega, r) = \frac{1}{a}\lim_{\varepsilon\to 0}[L_i(\omega, r) + M_i(\omega, r)], \qquad (2.67)$$

where each $L_i(\omega, r)$ is the contribution from the contour γ_1 and $M_i(\omega, r)$ is the contribution from the contour γ_ε in Fig. 1. We illustrate the procedure for calculating these by considering $L_1(\omega, r)$ and $M_1(\omega, r)$. The method works similarly for $K_2(\omega, r)$ and $K_3(\omega, r)$ but is more complicated.

Considering $L_1(\omega, r)$ first, we have

$$L_1(\omega, r) = \Re\left[\int_{\gamma_1} \frac{q}{(1-q^2)^{(3/2)}(1+e^{2\pi aq})}\,dq\right]$$

$$= \int_0^{1-\varepsilon} \frac{q}{(1-q^2)^{(3/2)}(1+e^{2\pi aq})}\,dq. \qquad (2.68)$$

Integrating by parts gives

$$L_1(\omega, r) = \frac{1}{2\sqrt{\varepsilon}(1+e^{2\pi a})} - \frac{1}{2}$$

$$+ 2\pi a \int_0^{1-\varepsilon} \frac{(1-q^2)^{-(1/2)}e^{2\pi aq}}{(1+e^{2\pi aq})^2}\,dq$$

$$+ O(\varepsilon^{(1/2)}). \qquad (2.69)$$

Note that the first term in (2.69) is divergent as $\varepsilon \to 0$, and that we have now isolated a finite integral (although the integrand is not regular). We next turn to $M_1(\omega, r)$:
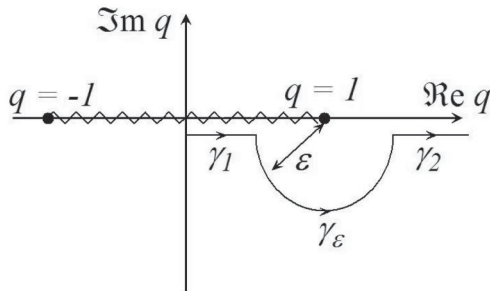

FIG. 1. Contour used for computing the integrals $K_i(\omega, r)$ (2.66).

$$M_1(\omega, r) = \Re\left[\int_{\gamma_\varepsilon} \frac{q}{(1-q^2)^{(3/2)}(1+e^{2\pi aq})}\,dq\right]. \quad (2.70)$$

Along γ_ε, we have

$$q - 1 = -\varepsilon e^{i\vartheta}, \qquad 0 < \vartheta < \pi. \qquad (2.71)$$

Changing the variable of integration in $M_1(\omega, r)$ to ϑ, and computing the integral, we find

$$M_1(\omega, r) = -\frac{1}{2\sqrt{\varepsilon}(1+e^{2\pi a})} + O(\varepsilon^{(1/2)}). \qquad (2.72)$$

Therefore, adding $L_1(\omega, r)$ and $M_1(\omega, r)$ will give a finite quantity and we can take the limit $\varepsilon \to 0$. It is helpful for numerical computation to integrate by parts again to give a regular integrand:

$$K_1(\omega, r) = -\frac{1}{2a} + \frac{\pi^2 e^{2\pi a}}{(1+e^{2\pi a})^2}$$

$$+ 4\pi^2 \int_0^a \sin^{-1}\left(\frac{\lambda}{a}\right)\frac{e^{2\pi\lambda}(e^{2\pi\lambda}-1)}{(1+e^{2\pi\lambda})^3}\,d\lambda, \quad (2.73)$$

where we have returned to the original variable $\lambda = aq$.

The calculation proceeds similarly for $K_2(\omega, r)$ and $K_3(\omega, r)$, except that more integrations by parts are required. In each case, the divergences in $L_i(\omega, r)$ and $M_i(\omega, r)$ cancel to give the following finite quantities:

$$K_2(\omega, r) = -\frac{1}{6a} + \frac{8\pi^3 a}{3}\int_0^a \left(1-\frac{\lambda^2}{a^2}\right)^{(1/2)}$$

$$\times \frac{e^{2\pi\lambda}(-1-e^{4\pi\lambda}+4e^{2\pi\lambda})}{(1+e^{2\pi\lambda})^4}\,d\lambda; \quad (2.74)$$

$$K_3(\omega, r) = -\frac{1}{10a} - \frac{16\pi^4 a}{15}\int_0^a \lambda\left(1-\frac{\lambda^2}{a^2}\right)^{(1/2)}$$

$$\times \frac{e^{2\pi\lambda}(-1+11e^{2\pi\lambda}-11e^{4\pi\lambda}+e^{6\pi\lambda})}{(1+e^{2\pi\lambda})^5}\,d\lambda. \quad$$

$$(2.75)$$

It is straightforward to verify that, for each i, the integrals $K_i(\omega, r)$ are $O(\omega^{-3})$ for large ω, so that the sums over n required in (2.58) will converge rapidly.

At this stage it is helpful to bring together our results for $\langle\phi^2\rangle_{\text{numeric}}$. From (2.58) we have

$$\langle\phi^2\rangle_{\text{numeric}} = \Sigma + \frac{T}{2\pi}\sum_{n=1}^\infty [J_0(\omega, r) + J_1(\omega, r)], \quad (2.76)$$

where

$$\Sigma = \frac{T}{2\pi} \sum_{n=1}^{\infty} \left\{ \sum_{\ell=0}^{\infty} (2\ell + 1)[C_{\omega\ell} p_{\omega\ell}(r) q_{\omega\ell}(r) - \beta_{0\omega\ell}(r) \right.$$

$$\left. - \beta_{1\omega\ell}(r)] \right\} + \frac{T}{4\pi} \left\{ \sum_{\ell=0}^{\infty} (2\ell + 1)[C_{0\ell} p_{0\ell}(r) q_{0\ell}(r) \right.$$

$$\left. - \beta_{00\ell}(r) - \beta_{10\ell}(r)] - \frac{\pi^2 r^3}{64 f^{(1/2)}} A_1 \right\}, \qquad (2.77)$$

and the numerical integrals $J_0(\omega, r)$ and $J_1(\omega, r)$ are given by (2.64) and (2.65), respectively, [with the $K_i(\omega, r)$ given by (2.73), (2.74), and (2.75)]. In the following we shall refer to Σ as the "mode sum."

III. NUMERICAL RESULTS FOR LUKEWARM BLACK HOLES

We now turn to the computation of $\langle\phi^2\rangle_{\rm ren}$ for a specific example, namely, lukewarm black holes [20]. We briefly review the key features of these black holes before describing the results of our calculation. For many of our numerical computations we have used standard routines [29]. Therefore we omit much of the detail of the numerical methods used, which are comprehensively discussed in Ref. [30].

A. Lukewarm black holes

Lukewarm black holes are a particular type of Reissner-Nordström−de Sitter space-time, with metric given by (2.2) and (2.3) with $M = Q$. For $4M < \sqrt{3/\Lambda}$, there are three distinct horizons [a black hole event horizon at $r = r_+$, an inner (Cauchy) horizon at $r = r_-$ and a cosmological horizon at $r = r_c$], given by

$$r_- = \frac{L}{2}\left[-1 + \sqrt{1 + \frac{4M}{L}} \right];$$

$$r_+ = \frac{L}{2}\left[1 - \sqrt{1 - \frac{4M}{L}} \right]; \qquad (3.1)$$

$$r_c = \frac{L}{2}\left[1 + \sqrt{1 - \frac{4M}{L}} \right];$$

where

$$L = \sqrt{\frac{3}{\Lambda}}, \qquad 4M < L. \qquad (3.2)$$

The Penrose diagram for this space-time can be found in [19].

In this case the event and cosmological horizons have equal surface gravities:

$$\kappa_+ = \kappa_c = \frac{1}{L}\sqrt{1 - \frac{4M}{L}}, \qquad (3.3)$$

which means that they have the same temperature $T = $

$\kappa_+/2\pi$. Here we are interested in the region between the event and cosmological horizons, which has a regular Euclidean section, with topology $S^2 \times S^2$ [19]. Our computations are for a thermal state at the natural temperature T.

In the following sections, we show plots of the constituent parts of $\langle\phi^2\rangle_{\rm ren}$ for the specific case of $M = Q = 0.1L$, although the main features are the same for other values of M. For the remainder of this section, all dimensionful quantities (r, M, etc.) are given in units of L.

B. Mode sum

We begin our numerical analysis by calculating the mode sum (2.77). First we need to find the modes themselves, by integrating the mode equation (2.10) which is satisfied by $p_{\omega\ell}(r)$ and $q_{\omega\ell}(r)$. This is done using standard shooting techniques [29].

The mode equation (2.10) has regular singular points at the event and cosmological horizons. Using the standard Frobenius method, we write the mode functions as power series:

$$S_{\omega\ell} = \sum_{i=0}^{\infty} a_i x^{i+\nu}, \qquad (3.4)$$

where $S_{\omega\ell}$ is either $p_{\omega\ell}(r)$ or $q_{\omega\ell}(r)$, and $x = r - r_+ > 0$ if we are considering the behavior near the event horizon ($x = r_c - r > 0$ if we are considering the behavior near the cosmological horizon). By looking at the lowest order term in (2.10) we obtain the indicial equation [15]:

$$\nu^2 = \omega^2 \left(\frac{df}{dr} \bigg|_{r=r_0} \right)^{-2}, \qquad (3.5)$$

where r_0 is either r_+ or r_c as applicable. In our mode sum (2.77), we are only summing over modes for which

$$\omega = 2\pi n T = n\kappa_+ = \frac{n}{2} \frac{df}{dx} \bigg|_{r=r_0}, \qquad n = 0, 1, 2, \dots \qquad (3.6)$$

Therefore $\nu = \pm n/2$, and the roots of the indicial equation differ by an integer ($n > 0$) or zero ($n = 0$). Therefore the linearly independent solutions of the mode equation (2.10) are

$$S_{1\omega\ell} = \sum_{i=0}^{\infty} a_i x^{i+(n/2)};$$

$$S_{2\omega\ell} = \sum_{i=0}^{\infty} b_i x^{i-(n/2)} + \mathcal{K}_{\omega\ell} S_{1\omega\ell} \ln\left(\frac{x}{r_0} \right); \qquad (3.7)$$

where $\mathcal{K}_{\omega\ell}$ is a constant which definitely does not vanish if $n = 0$ but may possibly vanish if $n > 0$, and $r_0 = r_+$ or r_c as applicable. The mode functions are chosen so that $p_{\omega\ell}$ is regular (that is, has the form $S_{1\omega\ell}$) near the event horizon, while $q_{\omega\ell}$ is regular near the cosmological horizon. From (3.7), it is clear that $q_{\omega\ell}$ will diverge (that is,

have the form $S_{2\omega\ell}$) near the event horizon, and $p_{\omega\ell}$ will diverge near the cosmological horizon. This can be seen in the examples of mode functions plotted in Fig. 2.

For $n > 0$, it is clear that the mode functions $p_{\omega\ell}(r)$ will vanish at the event horizon and that $q_{\omega\ell}(r)$ will vanish at the cosmological horizon. However, for $n = 0$, we have that $p_{0\ell}(r)$ is regular but nonzero at the event horizon [and similarly for $q_{0\ell}(r)$ at the cosmological horizon]. In this case $p_{0\ell}(r)$ will still diverge at the cosmological horizon because of the $\ln(x/r_0)$ term in $S_{2\omega\ell}$ (3.7) (note that $\mathcal{K}_{0\ell}$ cannot be zero because there must be two linearly independent solutions of the mode equation). It is straightforward to show, from the mode equation (2.10), that the mode functions are monotonic and do not have zeros except possibly at a horizon.

To find the $p_{\omega\ell}(r)$ mode functions, we start the numerical integration of the mode equation (2.10) just outside the event horizon, using as many terms in the power series expansion (3.7) of $S_{1\omega\ell}$ as required for the desired accuracy. As in [15], there is a complicated recurrence relation (involving seven terms in general) for the coefficients in the power series expansion (3.7), which we do not reproduce here. Starting with $a_0 = 1$, this recurrence relation is used to compute the power series expansion. We then integrate outwards towards the cosmological horizon. For the $q_{\omega\ell}(r)$ mode functions, we start integrating just inside the cosmological horizon, and integrate towards the event horizon. We use the Bulirsch-Stoer method [29] of integrating the differential equation (2.10) because the mode functions are not oscillating and because of the high degree of accuracy required.
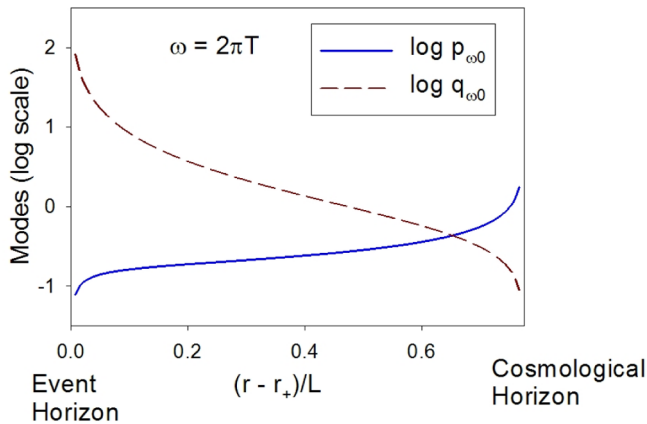

FIG. 2 (color online). Examples of mode solutions of the Eq. (2.10), with $\omega = 2\pi T$ and $\ell = 0$. The function $p_{\omega\ell}(r)$ vanishes at the event horizon (at the left-hand edge of the plot) and diverges at the cosmological horizon (at the right-hand edge of the plot), while the mode function $q_{\omega\ell}(r)$ vanishes at the cosmological horizon and diverges at the event horizon. For these mode functions, we have taken the scalar field to be massless and conformally coupled, and the black hole metric (2.2) and (2.3) has parameter $M = Q = 0.1L$. The radial coordinate on the horizontal axis is in units of L.

Looking at the mode sum (2.77), it can be seen that for large ω or ℓ, the rapid convergence of the sum is dependent on subtracting very nearly equal quantities. Therefore it is imperative to calculate the mode functions $p_{\omega\ell}(r)$, $q_{\omega\ell}(r)$ with great accuracy. We therefore used quadruple precision throughout our calculations. The normalization constant $C_{\omega\ell}$ is computed from (2.12). The constancy of the $C_{\omega\ell}$ as calculated from (2.12) for different values of r represents a good check on the accuracy of our results. For the particular case of $Q = M = 0.1L$, we find that $C_{\omega\ell}$ remains constant to within $10^{-26}|C_{\omega\ell}|$ for $0 \le n \le 25$ and $0 \le \ell \le 600$, which gives us enough modes to get good convergence of the mode sum (2.77).

Once we have the mode functions $p_{\omega\ell}(r)$, $q_{\omega\ell}(r)$, as the WKB approximants $\beta_{0\omega\ell}(r)$ (2.45) and $\beta_{1\omega\ell}(r)$ (2.46) are known analytically, we are able to find the mode sum (2.77). We found that the summand was $O(\ell^{-4})$ for large ℓ as predicted in Sec. II D. We found that the sums converged more quickly if we summed over n first and then ℓ. Convergence of the sums was speeded up by using a Shanks transformation (see appendix D of [3]). The disadvantage of the Shanks transformation is that one loses accuracy (typically the accuracy after the transformation is half that before), but we are nonetheless confident that our final answers are accurate to five significant figures. The form of the mode sum (2.77) will be shown explicitly as a function of r in Sec. III D.

C. Numerical integrals

The remainder of $\langle\phi^2\rangle_{\text{numeric}}$ involves sums of integrals which have to be computed numerically (2.76):

$$\langle\phi^2\rangle_{\text{numeric}}^{II} = \frac{T}{2\pi} \sum_{n=1}^{\infty} [J_0(\omega, r) + J_1(\omega, r)], \qquad (3.8)$$

where $J_0(\omega, r)$ is given by (2.64) and $J_1(\omega, r)$ is given in (2.65) as a combination of three integrals, $K_1(\omega, r)$ (2.73), $K_2(\omega, r)$ (2.74), and $K_3(\omega, r)$ (2.75). Each of these integrals depends on a (2.61), which in turn depends on $\omega = 2\pi nT$, for $n = 1, \ldots$ (note that the numerical integrals are only relevant for $\omega \neq 0$, as the modes for $\omega = 0$ were considered separately in Sec. II D). For each value of n, the integrals are straightforward to compute, and then summed over as many n as required for convergence. The summands are all $O(n^{-3})$ as $n \to \infty$ so convergence is relatively rapid. As an example of our results, we plot in Fig. 3

$$\sum_{n=1}^{\infty} K_i(\omega, r) \qquad (3.9)$$

for $i = 1, 2, 3$, showing how these sums vary with r.

From (2.73), (2.74), and (2.75), these sums are independent of the mass or coupling of the scalar field, but do depend on the metric of the black hole through the function f (2.3). It can be clearly seen in Fig. 3 that all three sums vanish at both the event and cosmological horizons. We
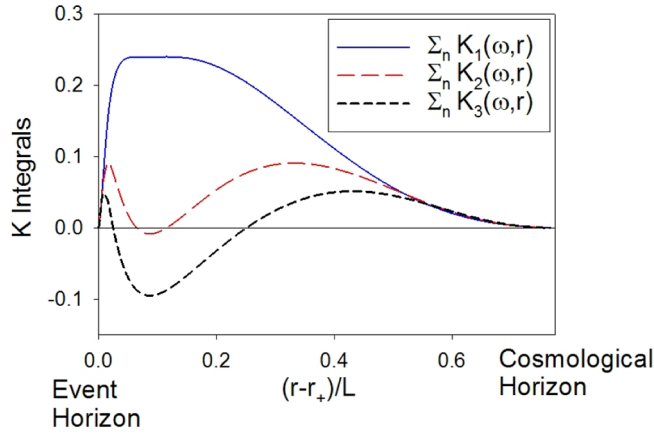
FIG. 3 (color online). Sums over n of the $K_i(\omega, r)$ integrals (2.73), (2.74), and (2.75) as functions of r. Note that these are independent of the mass or coupling of the scalar field. The radial coordinate on the horizontal axis is in units of L, and we consider the black hole metric (2.2) and (2.3) with parameter $M = Q = 0.1L$. It can be seen that all three sums vanish at the event horizon (left-hand edge of the plot) and the cosmological horizon (right-hand edge of the plot). This is in agreement with analytic work to be presented in Sec. IVA.

will show analytically in Sec. IVA that this is always the case, independent of the temperature of the thermal state under consideration.

D. Final answers

The final answers for $\langle \phi^2 \rangle_{\text{ren}}$ are now computed by combining the mode sum (2.77) with the numerical integral contribution (3.8) to give $\langle \phi^2 \rangle_{\text{numeric}}$ (2.38), and then adding this to $\langle \phi^2 \rangle_{\text{analytic}}$ (2.37).

We begin this section by examining the contributions to $\langle \phi^2 \rangle_{\text{numeric}}$, namely, the mode sum (2.77), and the two sums over numerical integrals

$$\frac{T}{2\pi} \sum_{n=1}^{\infty} J_0(\omega, r), \qquad \frac{T}{2\pi} \sum_{n=1}^{\infty} J_1(\omega, r). \qquad (3.10)$$

These are shown in Figs. 4–7 for a lukewarm black hole with $M = Q = 0.1L$. The quantity labeled "Total" in Figs. 4–7 is $\langle \phi^2 \rangle_{\text{numeric}}$.

In Figs. 4 and 5 we consider a massless, conformally coupled, scalar field, while in Figs. 6 and 7 the field is still conformally coupled but has mass $m = L$. We have chosen a large value of the mass so that the differences between this and the massless case are very clear.

Examining first the massless case, from Fig. 4 we can see that all three contributions to $\langle \phi^2 \rangle_{\text{numeric}}$ have peaks near the event horizon of the black hole, and that all three parts become very small at the cosmological horizon. The behavior near the event horizon is clearer in the close-up in Fig. 5. From Fig. 5 it can be seen that the contributions coming from sums over the numerical integrals (3.10) tend
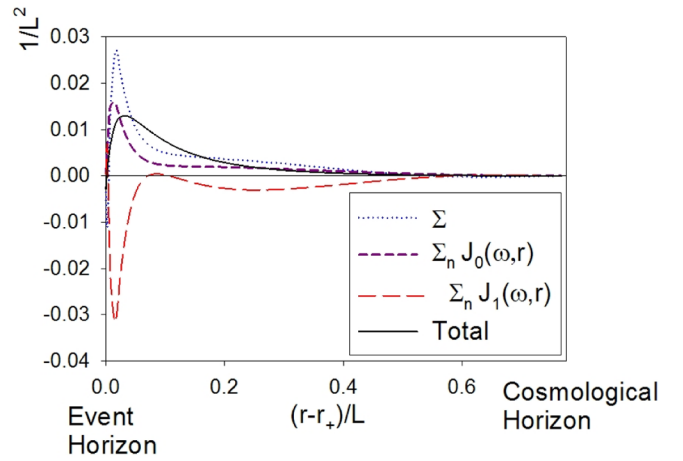

FIG. 4 (color online). Contributions to $\langle \phi^2 \rangle_{\text{numeric}}$ (2.38) from the mode sum Σ (2.77) and the sums over the numerical integrals (3.10), as functions of r. Here, the quantum scalar field is massless and conformally coupled. The radial coordinate on the horizontal axis is in units of L, and the black hole metric (2.2) and (2.3) has parameter $M = Q = 0.1L$. All quantities appear to be regular near the cosmological horizon. Their behavior near the event horizon is shown in close-up in Fig. 5.

to zero as the horizon is approached, and the dominant contribution to $\langle \phi^2 \rangle_{\text{numeric}}$ comes from the mode sum Σ (2.77). Furthermore, this appears to remain finite as the horizon is approached.

When the scalar field is no longer massless, we see the difference in behavior clearly in Fig. 6. Near the cosmological horizon, the contributions to $\langle \phi^2 \rangle_{\text{numeric}}$ from the sums over the numerical integrals (3.10) still vanish as the horizon is approached, but now the mode sum Σ (2.77)
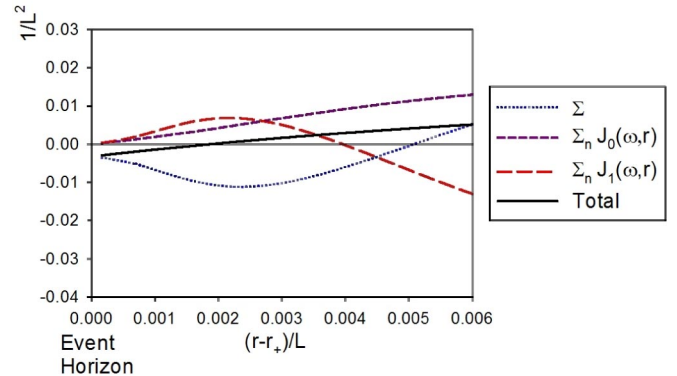

FIG. 5 (color online). Close-up, near the event horizon, of the contributions (shown in Fig. 4) to $\langle \phi^2 \rangle_{\text{numeric}}$ (2.38) from the mode sum Σ (2.77) and the sums over the numerical integrals (3.10), when the quantum scalar field is massless and conformally coupled. It is clear that the contributions from the sums over the numerical integrals (3.10) vanish at the event horizon. Near the horizon the mode sum Σ (2.77) is the dominant contribution and this appears to remain finite as the horizon is approached.
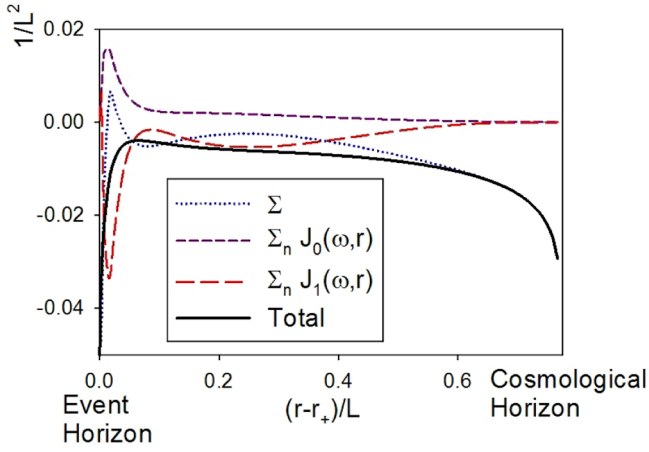
FIG. 6 (color online). Contributions to $\langle\phi^2\rangle_{\mathrm{numeric}}$ (2.38) from the mode sum Σ (2.77) and the sums over the numerical integrals (3.10), as functions of r. Here, the quantum scalar field is conformally coupled but has mass $m = L$. The radial coordinate on the horizontal axis is in units of L, and the black hole metric (2.2) and (2.3) has parameter $M = Q = 0.1L$. The contributions from the sums over the numerical integrals appear to be regular near the cosmological horizon, but the mode sum Σ (2.77) is diverging as the cosmological horizon is approached. The behavior of these quantities near the event horizon is shown in close-up in Fig. 7.

(and therefore $\langle\phi^2\rangle_{\mathrm{numeric}}$) diverges. The close-up near the event horizon in Fig. 7 confirms that this also happens near the black hole event horizon.

We will show in Sec. IV that the contributions to $\langle\phi^2\rangle_{\mathrm{numeric}}$ from the sums over numerical integrals always vanish at the horizons, whatever the mass or coupling of the scalar field, so that the mode sum Σ is indeed the
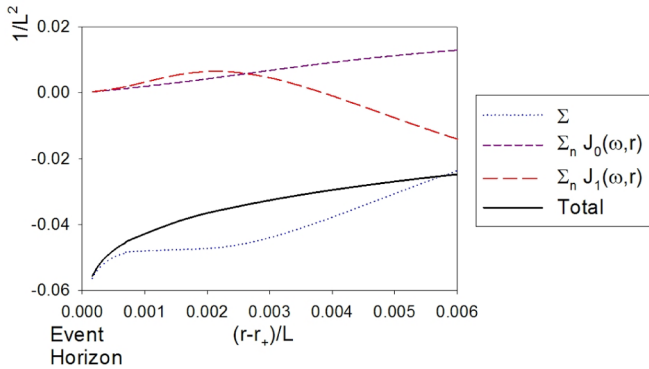

FIG. 8 (color online). The vacuum polarization $\langle\phi^2\rangle_{\mathrm{ren}}$ and its components $\langle\phi^2\rangle_{\mathrm{analytic}}$ (2.37) and $\langle\phi^2\rangle_{\mathrm{numeric}}$ (2.38) (all in units of L^{-2}). Here, the quantum scalar field is massless and conformally coupled. The radial coordinate on the horizontal axis is in units of L, and the black hole metric (2.2) and (2.3) has parameter $M = Q = 0.1L$. All quantities appear to be finite near both the event and cosmological horizons. Near the event and cosmological horizons, $\langle\phi^2\rangle_{\mathrm{analytic}}$ is the dominant contribution to $\langle\phi^2\rangle_{\mathrm{ren}}$.

dominant contribution to $\langle\phi^2\rangle_{\mathrm{numeric}}$ near the horizons. Furthermore, we will show that Σ diverges near a horizon unless the quantum scalar field is both massless and conformally coupled.

We now turn to the final result, namely, $\langle\phi^2\rangle_{\mathrm{ren}}$. In Figs. 8 and 9 we plot $\langle\phi^2\rangle_{\mathrm{analytic}}$ (2.37), $\langle\phi^2\rangle_{\mathrm{numeric}}$ (2.38), and their sum $\langle\phi^2\rangle_{\mathrm{ren}}$ for a massless, conformally coupled scalar field, and a conformally coupled scalar field with mass $m = L$.

FIG. 7 (color online). Close-up, near the event horizon, of the contributions (shown in Fig. 6) to $\langle\phi^2\rangle_{\mathrm{numeric}}$ (2.38) from the mode sum Σ (2.77) and the sums over the numerical integrals (3.10), when the quantum scalar field is conformally coupled and has mass $m = L$. It is clear that the contributions from the sums over the numerical integrals (3.10) vanish at the event horizon. Near the horizon the mode sum Σ (2.77) is the dominant contribution and this appears to be diverging as the horizon is approached.
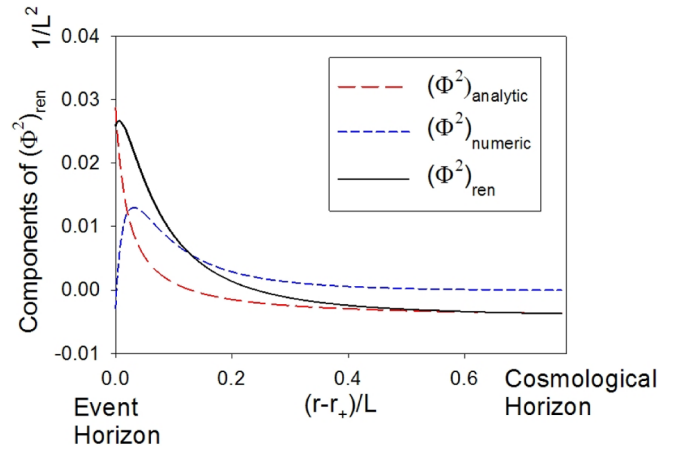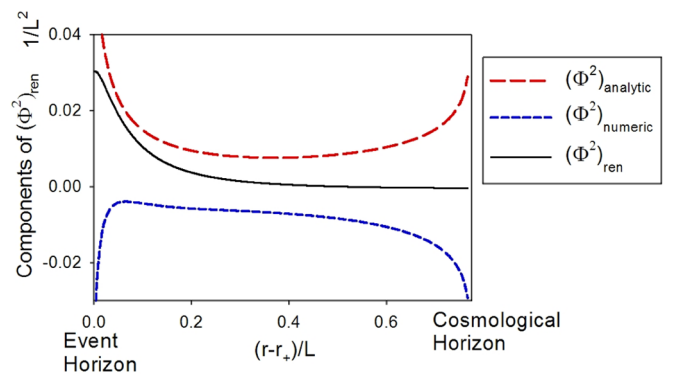

FIG. 9 (color online). The vacuum polarization $\langle\phi^2\rangle_{\mathrm{ren}}$ and its components $\langle\phi^2\rangle_{\mathrm{analytic}}$ (2.37) and $\langle\phi^2\rangle_{\mathrm{numeric}}$ (2.38) (all in units of L^{-2}). Here, the quantum scalar field is conformally coupled and has mass $m = L$. The radial coordinate on the horizontal axis is in units of L, and the black hole metric (2.2) and (2.3) has parameter $M = Q = 0.1L$. It can be clearly seen that both $\langle\phi^2\rangle_{\mathrm{analytic}}$ and $\langle\phi^2\rangle_{\mathrm{numeric}}$ diverge near the event and cosmological horizons, but with opposite signs.

When the scalar field is massless and conformally coupled, from Fig. 8 it is clear that $\langle\phi^2\rangle_{\text{analytic}}$, $\langle\phi^2\rangle_{\text{numeric}}$, and $\langle\phi^2\rangle_{\text{ren}}$ are regular at both the event and cosmological horizons. The total $\langle\phi^2\rangle_{\text{ren}}$ is greatest near the event horizon, and slightly negative near the cosmological horizon. The contribution $\langle\phi^2\rangle_{\text{analytic}}$ has the same qualitative behavior as the total $\langle\phi^2\rangle_{\text{ren}}$ but does not represent more than a qualitative approximation to the exact quantity.

When the quantum scalar field is not massless, from Fig. 9 we can see that both $\langle\phi^2\rangle_{\text{analytic}}$ and $\langle\phi^2\rangle_{\text{numeric}}$ diverge as either the event or cosmological horizons are approached, albeit with opposite signs. From our numerical results, it looks like these divergences cancel to give a finite $\langle\phi^2\rangle_{\text{ren}}$. However, finiteness of this quantity cannot be proven by numerical calculations alone. Therefore, in the next section, we study $\langle\phi^2\rangle_{\text{ren}}$ analytically.

IV. REGULARITY ON THE HORIZONS

Our numerical results, computed in the previous section, indicate that $\langle\phi^2\rangle_{\text{ren}}$ is finite on both the event and cosmological horizons, for the thermal state at the same temperature as both horizons. In this section we shall show analytically that this is indeed the case. We shall consider a general, nonextremal horizon at $r = r_0$, and show that $\langle\phi^2\rangle_{\text{ren}}$ is regular at that horizon for a thermal state at the same temperature as the horizon.

A. Analytic part and numerical integrals

We consider first the behavior of $\langle\phi^2\rangle_{\text{analytic}}$ at a horizon $r = r_0$. In order to analyze the regularity at a horizon of $\langle\phi^2\rangle_{\text{analytic}}$ (2.37), we split it into two parts:

$$\langle\phi^2\rangle_{\text{analytic}} = \langle\phi^2\rangle^I_{\text{analytic}} + \langle\phi^2\rangle^{II}_{\text{analytic}}; \qquad (4.1)$$

where

$$\langle\phi^2\rangle^I_{\text{analytic}} = \frac{m^2}{16\pi^2} - \frac{1}{192\pi^2 f}\left(\frac{df}{dr}\right)^2 + \frac{1}{96\pi^2}\frac{d^2f}{dr^2}$$
$$+ \frac{1}{48\pi^2 r}\frac{df}{dr} + \frac{\kappa^2}{48\pi^2 f};$$

$$\langle\phi^2\rangle^{II}_{\text{analytic}} = -\frac{1}{8\pi^2}\left[m^2 + \left(\xi - \frac{1}{6}\right)R\right]$$
$$\times \left[C + \frac{1}{2}\ln\left(\frac{\mu^2 f}{4\kappa^2}\right)\right]. \qquad (4.2)$$

At first sight it looks like $\langle\phi^2\rangle^I_{\text{analytic}}$ is divergent at a horizon where $f = 0$, but in fact it is straightforward to show that if κ is chosen to be $\frac{1}{2}\frac{df}{dr}$ at the horizon, then $\langle\phi^2\rangle^I_{\text{analytic}}$ is regular there. This is in accordance with expectations: if the temperature $T = 2\pi\kappa$ of the state matches the natural temperature of the horizon we are considering, then $\langle\phi^2\rangle^I_{\text{analytic}}$ is regular at that horizon. In particular, for the lukewarm black holes, we have that

$\langle\phi^2\rangle^I_{\text{analytic}}$ is regular at both the event and cosmological horizons.

On the other hand, it is clear that $\langle\phi^2\rangle^{II}_{\text{analytic}}$ has a logarithmic divergence as $f \to 0$ unless both $m^2 = 0$ and $\xi = 1/6$, that is, the field is massless and conformally coupled. We will show in the next subsection that this divergence cancels with a corresponding divergence in the mode sum Σ (2.77), to give an overall $\langle\phi^2\rangle_{\text{ren}}$ which is regular.

Before that, we examine next the other contribution to $\langle\phi^2\rangle_{\text{numeric}}$, namely,

$$\langle\phi^2\rangle^{II}_{\text{numeric}} = \frac{T}{2\pi}\sum_{n=1}^{\infty}[J_0(\omega, r) + J_1(\omega, r)], \qquad (4.3)$$

where $J_0(\omega, r)$ and $J_1(\omega, r)$ are given, respectively, by (2.64) and (2.65), with $J_1(\omega, r)$ in turn determined by the integrals in (2.73), (2.74), and (2.75). It is straightforward to show that, for fixed ω and small f, the integrals $J_0(\omega, r)$, $K_1(\omega, r)$, $K_2(\omega, r)$, and $K_3(\omega, r)$ behave as follows:

$$J_0(\omega, r) = \frac{7f}{1920\omega^3 r_0^4} + O(f^2);$$

$$K_1(\omega, r) = \frac{f^{(3/2)}}{48\omega^3 r^3} + \frac{21f^{(5/2)}}{3840\omega^5 r_0^5} + O(f^{(7/2)});$$

$$K_2(\omega, r) = \frac{f^{(3/2)}}{48\omega^3 r^3} + \frac{7f^{(5/2)}}{768\omega^5 r_0^5} + O(f^{(7/2)}); \qquad (4.4)$$

$$K_3(\omega, r) = \frac{f^{(3/2)}}{48\omega^3 r^3} + \frac{49f^{(5/2)}}{3840\omega^5 r_0^5} + O(f^{(7/2)});$$

where $r = r_0$ is the location of the horizon where $f = 0$. We should comment that the first terms in the expansions of $K_1(\omega, r)$, $K_2(\omega, r)$, and $K_3(\omega, r)$ do have r and not r_0 in the denominator. Therefore they include some second order terms as well as leading order terms. Writing the expansions in this way simply makes the expressions shorter. From (4.4), it is clear that the sums over the $K_i(\omega, r)$ should vanish at the horizon, regardless of the temperature T of the state under consideration or the mass or coupling of the scalar field. This is in agreement with our numerical results in Fig. 3.

Combining the $K_i(\omega, r)$ integrals to form $J_1(\omega, r)$ using (2.65), we find that the leading order contributions from the $K_i(\omega, r)$ integrals cancel and $J_1(\omega, r)$ has the following behavior:

$$J_1(\omega, r) = \frac{7f}{7680\omega^5 r_0^4}\left(\frac{df}{dr}\right)^2 + O(f^2). \qquad (4.5)$$

Recalling that $\omega = 2n\pi T$, $n \neq 0$, we therefore see that both $J_0(\omega, r)$ and $J_1(\omega, r)$ tend to zero uniformly in n as $f \to 0$, and therefore the contributions to $\langle\phi^2\rangle_{\text{numeric}}$ from the numerical integrals (4.3) vanish at both the event and cosmological horizons. This is independent of the (nonzero) temperature of the state under consideration, and the

mass and curvature coupling of the scalar field, and is in agreement with our numerical results in Figs. 4–7.

Therefore the only parts of $\langle\phi^2\rangle_{\text{ren}}$ which need further investigation are $\langle\phi^2\rangle^{II}_{\text{analytic}}$ (4.2), which has a logarithmic divergence as $r \rightarrow r_0$, and the mode sum (2.77) contribution to $\langle\phi^2\rangle_{\text{numeric}}$. If $\langle\phi^2\rangle_{\text{ren}}$ is to be regular at the horizon, it must be the case that the mode sum Σ (2.77) also has a logarithmic divergence, and, furthermore, this must exactly cancel the logarithmic divergence in $\langle\phi^2\rangle^{II}_{\text{analytic}}$. We next establish that this is the case using a careful analysis of the mode functions.

B. Mode sums

The behavior of the mode sum Σ (2.77) near a horizon is by far the most difficult part of $\langle\phi^2\rangle_{\text{ren}}$ to analyze. The reason for this is that the sums over ℓ are not uniformly convergent: more and more ℓ's are needed before convergence is reached as we get closer and closer to a horizon. This is due to the fact that the WKB approximants $\beta_{0\omega\ell}(r)$ (2.45) and $\beta_{1\omega\ell}(r)$ (2.46) do not depend on ℓ when $f = 0$, as in this case $\chi_{\omega\ell}(r)$ (2.42) reduces to

$$\chi_{\omega\ell}(r) = \omega r^2. \tag{4.6}$$

Furthermore, the WKB approximants do not correctly reproduce the $\ln[(r - r_0)/r_0]$ behavior seen in the field modes (3.7) near the horizon.

Suppose we are considering a horizon on which the mode functions $p_{\omega\ell}(r)$ are regular and the $q_{\omega\ell}(r)$ diverge. The analysis below will be equally valid if we are on a horizon where the $p_{\omega\ell}(r)$ diverge and the $q_{\omega\ell}(r)$ are regular, but with the p's and q's swapped over. Then near the horizon, the mode functions $p_{\omega\ell}(r)$ and $q_{\omega\ell}(r)$ will have the following behavior (3.7):

$$p_{\omega\ell}(r) = (r - r_0)^{(n/2)} + O(r - r_0)^{1+(n/2)};$$
$$q_{\omega\ell}(r) = (r - r_0)^{-(n/2)} + O(r - r_0)^{1-(n/2)}$$
$$+ \mathcal{K}_{\omega\ell}(r - r_0)^{(n/2)} \ln\left(\frac{r - r_0}{r_0}\right)$$
$$+ O\left[(r - r_0)^{1+(n/2)} \ln\left(\frac{r - r_0}{r_0}\right)\right]; \tag{4.7}$$

for some constant $\mathcal{K}_{\omega\ell}$, where $\omega = 2\pi n T$. Therefore, near the horizon, we have

$$C_{\omega\ell}p_{\omega\ell}(r)q_{\omega\ell}(r) \sim C_{\omega\ell}\mathcal{K}_{\omega\ell}(r - r_0)^n \ln\left(\frac{r - r_0}{r_0}\right)$$
$$+ \text{finite terms}. \tag{4.8}$$

From (4.8), it is clear that the only contribution to the mode sum Σ which is important near the horizon is that for $n = 0 = \omega$, since this contains a $\ln[(r - r_0)/r_0]$ term which diverges at the horizon. For $n > 0$, the $(r - r_0)^n \ln[(r - r_0)/r_0]$ term is subleading compared to the finite terms. The finite terms in (4.8) for $n > 0$ are described well by the conventional WKB approximation described in Sec. II D

and their contribution to the total mode sum is finite as the horizon is approached [23].

To analyze the behavior of the mode sum Σ, what is therefore required is an approximation for the mode functions with $n = \omega = 0$, near the horizon, which is *uniformly* valid in ℓ. Such an approximation was first developed by Candelas [5] for Schwarzschild black holes, and subsequently extended in Ref. [23] for the Reissner-Nordström black hole. Here we generalize the approach of Ref. [23] for general metric function $f(r)$. We focus on the case of a horizon at $r = r_0$, where $p_{0\ell}(r)$ is regular and $q_{0\ell}(r)$ diverges, but the analysis proceeds similarly for a horizon where $q_{0\ell}(r)$ is regular and $p_{0\ell}(r)$ diverges.

We begin by writing the mode functions in terms of modified Bessel functions [23]:

$$p_{0\ell}(r) = \left(\frac{\Gamma(r)}{r^2\Omega(r)}\right)^{(1/2)} I_0(\Gamma(r));$$
$$q_{0\ell}(r) = \left(\frac{\Gamma(r)}{r^2\Omega(r)}\right)^{(1/2)} K_0(\Gamma(r)); \tag{4.9}$$

where $\Gamma(r)$ and $\Omega(r)$ are functions which we shall define very shortly. The mode functions (4.9) are required to satisfy the differential equation (2.10) and the normalization condition (2.12). Considering the normalization condition (2.12) first, this is identically satisfied with $C_{0\ell} = 1$ if $\Gamma(r)$ is defined to be

$$\Gamma(r) = \int_{r'=r_0}^{r} \frac{\Omega(r')}{f(r')} dr', \tag{4.10}$$

whatever the (as yet undetermined) function $\Omega(r)$. With this definition of $\Gamma(r)$, substituting (4.9) into (2.10) gives a differential equation for $\Omega(r)$ which can be found in [23]. Following [23], the function $\Omega(r)$ is defined to be

$$\Omega(r) = y(r)\sqrt{f(r)}, \tag{4.11}$$

where $y(r)$ is a function which is regular at the horizon. To analyze the behavior of the mode functions near the horizon, we expand $f(r)$ and $y(r)$ near the horizon as follows:

$$f(r) = x[f_1 + xf_2 + O(x^2)];$$
$$y(r) = B[1 + xy_1 + x^2y_2 + O(x^3)]; \tag{4.12}$$

where f_i, B, and y_i are constants and $x = r - r_0$. The fact that this expansion should be *uniform* in ℓ means that the constants y_i must be bounded as $\ell \rightarrow \infty$. The expansions (4.12) lead to the following behavior near the horizon:

$$\Gamma(r) = \frac{2B}{r_0}\sqrt{\frac{x}{f_1}} + O(x^{(3/2)});$$
$$\left(\frac{\Gamma(r)}{r^2\Omega(r)}\right)^{(1/2)} = \sqrt{\frac{2}{f_1 r_0^2}} + O(x). \tag{4.13}$$

The expansions (4.12) are substituted, in turn, into (4.11), then (4.10) and finally (4.9) to give the form of

the mode functions near the horizon. These are then, in turn, substituted into the mode equation (2.10), which is then expanded in powers of x. The lowest order term in (2.10) gives the following expression for the constant B:

$$B^2 = \ell(\ell + 1) + \tfrac{1}{3}r_0 f_1 + \tfrac{1}{3}r_0^2 f_1 y_1 + \tfrac{1}{3}$$
$$+ m^2 r_0^2 + (\xi - \tfrac{1}{6})R_0 r_0^2, \qquad (4.14)$$

where $R_0 = R(r_0)$ is the value of the Ricci scalar on the horizon. The expression (4.14) generalizes that found in [23] for the Reissner-Nordström case. As in [23], the next-to-leading order term in the mode equation (2.10) gives a complicated expression involving y_1 and y_2. Using the fact that both y_1 and y_2 must remain bounded as $\ell \to \infty$, we obtain

$$y_1 = -\frac{1}{r_0} + O(\ell^{-2}) \quad \text{as } \ell \to \infty, \qquad (4.15)$$

which means that, as $\ell \to \infty$, we have

$$B^2 = \ell(\ell + 1) + \tfrac{1}{3} + m^2 r_0^2 + (\xi - \tfrac{1}{6})R_0 r_0^2 + O(\ell^{-2}). \qquad (4.16)$$

We may now use the form of the mode functions (4.9) to study the contribution of the $\omega = 0$ modes to the mode sum Σ (2.77) near the horizon. In other words, we wish to analyze

$$\Sigma_0 = \frac{T}{4\pi} \sum_{\ell=0}^{\infty} \left[(2\ell + 1)C_{0\ell} p_{0\ell}(r) q_{0\ell}(r) - \frac{1}{rf^{(1/2)}} \right]$$
$$= \frac{T}{4\pi} \sum_{\ell=0}^{\infty} \left[(2\ell + 1)\left(\frac{\Gamma(r)}{r^2\Omega(r)}\right)I_0(\Gamma(r))K_0(\Gamma(r)) \right.$$
$$\left. - \frac{1}{rf^{(1/2)}} \right]. \qquad (4.17)$$

In Sec. II D, we added and subtracted $\sum_{\ell=0}^{\infty} \beta_{10\ell}(r)$ to this sum to give a sum which was more readily computed numerically. We do not need to do this here as the sum is convergent. In addition, $\beta_{10\ell}(r)$ diverges as $r \to r_0$, so that the sum (4.17) is more straightforward to analyze, as it does not include these additional divergences (which do, however, cancel).

Using the Watson-Sommerfeld formula (2.55), we convert the sum (4.17) over ℓ into two integrals:

$$\Sigma_0 = \frac{T}{4\pi}[\Sigma_0^I + \Sigma_0^{II}], \qquad (4.18)$$

where

$$\Sigma_0^I = \int_0^{\infty} d\lambda \left[2\lambda\left(\frac{\Gamma(r)}{r^2\Omega(r)}\right)I_0(\Gamma(r))K_0(\Gamma(r)) - \frac{1}{rf^{(1/2)}} \right]; \qquad (4.19)$$

$$\Sigma_0^{II} = -\Re\left\{ i \int_0^{\infty} d\lambda \frac{2}{1 + e^{2\pi\lambda}} \right.$$
$$\left. \times \left[2i\lambda\left(\frac{\Gamma(r)}{r^2\Omega(r)}\right)I_0(\Gamma(r))K_0(\Gamma(r)) - \frac{1}{rf^{(1/2)}} \right] \right\}. \qquad (4.20)$$

In (4.19) we have $\ell = \lambda - 1/2$, while in (4.20) we have $\ell = i\lambda - 1/2$. In both cases the functions $\Gamma(r)$ and $\Omega(r)$ depend on ℓ.

We now use the expansions (4.13) for the functions $\Gamma(r)$ and $\Omega(r)$ near the horizon, which are uniform in ℓ. It turns out that Σ_0^{II} is the more straightforward to work with, so we examine this first. Using (4.13), the leading order behavior of Σ_0^{II} near the horizon is given by

$$\Sigma_0^{II} = \Re\left\{ \int_0^{\infty} d\lambda \frac{8\lambda}{r_0^2 f_1(1 + e^{2\pi\lambda})} I_0\left(\frac{2B}{r_0}\sqrt{\frac{x}{f_1}}\right) \right.$$
$$\left. \times K_0\left(\frac{2B}{r_0}\sqrt{\frac{x}{f_1}}\right) \right\} + O(x\ln[x/r_0]), \qquad (4.21)$$

where B depends on λ. In this case we can use the approximate behavior of the modified Bessel functions for small x [31]:

$$I_0(x) = 1 + O(x^2);$$
$$K_0(x) = -C - \ln\left(\frac{x}{2}\right) + O(x^2 \ln x); \qquad (4.22)$$

where C is Euler's constant. We then obtain the following expression for Σ_0^{II}:

$$\Sigma_0^{II} = -\frac{1}{6r_0^2 f_1}\left[C + \ln\left(\frac{1}{r_0}\sqrt{\frac{x}{f_1}}\right) \right]$$
$$- \frac{8}{r_0^2 f_1}\Re\left\{ \int_0^{\infty} d\lambda \frac{\lambda}{1 + e^{2\pi\lambda}} \ln B \right\} + O\left[x\ln\left(\frac{x}{r_0}\right) \right]. \qquad (4.23)$$

The integral in (4.23) involving $\ln B$ cannot be computed exactly because we do not have a closed-form expression for B for all values of ℓ. However, this integral does not depend on x, and is finite because the behavior of B for large λ is given by (4.16). Therefore, we have, near the horizon,

$$\Sigma_0^{II} = -\frac{1}{12r_0^2 f_1}\ln\left(\frac{x}{r_0}\right) + \text{finite terms.} \qquad (4.24)$$

Next we consider Σ_0^I (4.19). From (4.14) with $\ell = \lambda - \tfrac{1}{2}$, we have

$$2B\frac{dB}{d\lambda} = 2\lambda + \frac{1}{3}r_0^2 f_1 \frac{dy_1}{d\lambda}, \qquad (4.25)$$

so that, for large λ,

$$2B\frac{dB}{d\lambda} = 2\lambda + O(\lambda^{-2}). \qquad (4.26)$$

Defining $B_0 = B(\lambda = 0)$, and using the expansions (4.13), the leading order behavior of Σ_0^I can be written as

$$\Sigma_0^I = \tilde{\Sigma}_1 + \tilde{\Sigma}_2 + O(x \ln[x/r_0]), \qquad (4.27)$$

where

$$\tilde{\Sigma}_1 = \int_{B_0}^{\infty} dB \left\{ \frac{4B}{r_0^2 f_1} I_0\left(\frac{2B}{r_0}\sqrt{\frac{x}{f_1}}\right) K_0\left(\frac{2B}{r_0}\sqrt{\frac{x}{f_1}}\right) - \frac{d\lambda}{dB} \frac{1}{r_0 \sqrt{f_1} x} \right\};$$

$$\tilde{\Sigma}_2 = \int_0^{\infty} d\lambda \left\{ \frac{4}{r_0^2 f_1} I_0\left(\frac{2B}{r_0}\sqrt{\frac{x}{f_1}}\right) K_0\left(\frac{2B}{r_0}\sqrt{\frac{x}{f_1}}\right) \left[\lambda - B \frac{dB}{d\lambda} \right] \right\}. \qquad (4.28)$$

To compute $\tilde{\Sigma}_1$, we first change the upper limit of the integral from $\lambda = \infty$ to $\lambda = \lambda_L \gg 1$, which simplifies the analysis. The integral $\tilde{\Sigma}_1$ is in fact regular as $\lambda_L \to \infty$, but the individual terms in it are not. We use the standard result [23], valid for all nonzero ν:

$$\int 2B I_0(B\nu) K_0(B\nu) dB = B^2 [I_0(B\nu) K_0(B\nu) + I_1(B\nu) K_1(B\nu)], \qquad (4.29)$$

which gives

$$\tilde{\Sigma}_1 = \left[\frac{2}{r_0^2 f_1} B^2 \left\{ I_0\left(\frac{2B}{r_0}\sqrt{\frac{x}{f_1}}\right) K_0\left(\frac{2B}{r_0}\sqrt{\frac{x}{f_1}}\right) + I_1\left(\frac{2B}{r_0}\sqrt{\frac{x}{f_1}}\right) K_1\left(\frac{2B}{r_0}\sqrt{\frac{x}{f_1}}\right) \right\} - \frac{\lambda(B)}{r_0\sqrt{f_1}x} \right]_{B_0}^{B_L}, \qquad (4.30)$$

where $B_L = B(\lambda_L)$. For large z, we then use the expansion [31]:

$$I_n(z) K_n(z) = \frac{1}{2z}\left[1 - \frac{4n^2 - 1}{8z^2} + O(z^{-4}) \right], \qquad (4.31)$$

together with the behavior of B for large ℓ (4.16). This enables us to simplify the expression (4.30) to obtain a quantity which is manifestly finite as $\lambda_L \to \infty$, and then we can take the limit $\lambda_L \to \infty$. The answer obtained is

$$\tilde{\Sigma}_1 = -\frac{2B_0^2}{r_0^2 f_1}\left[I_0\left(\frac{2B_0}{r_0}\sqrt{\frac{x}{f_1}}\right) K_0\left(\frac{2B_0}{r_0}\sqrt{\frac{x}{f_1}}\right) + I_1\left(\frac{2B_0}{r_0}\sqrt{\frac{x}{f_1}}\right) K_1\left(\frac{2B_0}{r_0}\sqrt{\frac{x}{f_1}}\right) \right]. \qquad (4.32)$$

For small x, we now expand $\tilde{\Sigma}_1$, using (4.22) and [31]

$$I_1(x) K_1(x) = \tfrac{1}{2} + O(x^2 \ln[x/r_0]), \qquad (4.33)$$

to give, for small x,

$$\tilde{\Sigma}_1 = \frac{B_0^2}{r_0^2 f_1} \ln\left(\frac{x}{r_0}\right) + \text{finite terms}. \qquad (4.34)$$

For $\tilde{\Sigma}_2$, it is sufficient to use the expansions (4.22) in the integrand to give, for small x,

$$\tilde{\Sigma}_2 = -\frac{2}{r_0^2 f_1} \ln\left(\frac{x}{r_0}\right) \int_0^{\infty} d\lambda \left(\lambda - B \frac{dB}{d\lambda}\right) + \text{finite terms}$$

$$= -\frac{1}{r_0^2 f_1}\left[B_0^2 - \frac{1}{12} - m^2 r_0^2 - \left(\xi - \frac{1}{6}\right) R_0 r_0^2 \right] \ln\left(\frac{x}{r_0}\right)$$

$$+ \text{finite terms}. \qquad (4.35)$$

Combining (4.34) and (4.35), we find the following expression for Σ_0^I (4.27):

$$\Sigma_0^I = \frac{1}{r_0^2 f_1}\left[\frac{1}{12} + m^2 r_0^2 + \left(\xi - \frac{1}{6}\right) R_0 r_0^2 \right] \ln\left(\frac{x}{r_0}\right)$$

$$+ \text{finite terms}, \qquad (4.36)$$

and, combining this with (4.24), gives our final expression for the behavior of the mode sum Σ (2.77) near the horizon:

$$\Sigma = \frac{T}{4\pi f_1}\left[m^2 + \left(\xi - \frac{1}{6}\right) R_0 \right] \ln\left(\frac{x}{r_0}\right) + \text{finite terms}$$

$$= \frac{1}{16\pi^2}\left[m^2 + \left(\xi - \frac{1}{6}\right) R_0 \right] \ln\left(\frac{x}{r_0}\right) + \text{finite terms}, \qquad (4.37)$$

where we have used the fact that the temperature $T = \kappa/2\pi$, where $\kappa = f_1/2$ is the surface gravity of the horizon.

From (4.37) we see that the mode sum Σ diverges near a horizon unless the quantum scalar field is massless and conformally coupled. This behavior can be seen in our numerical results in Figs. 4–7, where it is apparent that Σ is regular at a horizon in the massless, conformally coupled, case but otherwise divergent.

Finally, comparing (4.2) and (4.37), we see that the logarithmic divergences cancel and $\Sigma + \langle\phi^2\rangle_{\text{analytic}}^{II}$ is regular at the horizon. Since we have already shown that the remaining contributions to $\langle\phi^2\rangle_{\text{ren}}$, namely, $\langle\phi^2\rangle_{\text{analytic}}^{I}$ (4.2) and $\langle\phi^2\rangle_{\text{numeric}}^{II}$ (4.3), are regular at a horizon, we therefore conclude that the total $\langle\phi^2\rangle_{\text{ren}}$, for a thermal state at the same temperature as the horizon, is regular at that horizon. For the particular case of lukewarm black holes, the analysis above applies equally well to the event and cosmological horizons, which are at the same temperature. Therefore, for a thermal state at this temperature, we have shown analytically that $\langle\phi^2\rangle_{\text{ren}}$ is finite at both the event and cosmological horizons. This means that the divergences seen (Fig. 9) in $\langle\phi^2\rangle_{\text{analytic}}$ and $\langle\phi^2\rangle_{\text{numeric}}$ when the scalar field is no longer massless do in fact cancel to give a finite $\langle\phi^2\rangle_{\text{ren}}$.

V. CONCLUSIONS

In this paper we have studied the renormalized expectation value $\langle\phi^2\rangle_{\text{ren}}$ for a quantum scalar field on a lukewarm black hole background, where the space-time possesses a black hole event horizon and a cosmological horizon which are at the same temperature. We have used

the method of [1] to compute $\langle\phi^2\rangle_{\mathrm{ren}}$ for a thermal quantum state at this natural temperature. Our numerical computations have indicated that $\langle\phi^2\rangle_{\mathrm{ren}}$ is regular on both the event and cosmological horizons, and this has been proved analytically as well.

The method of Ref. [1] splits $\langle\phi^2\rangle_{\mathrm{ren}}$ into two parts, an analytic expression $\langle\phi^2\rangle_{\mathrm{analytic}}$ and a part, $\langle\phi^2\rangle_{\mathrm{numeric}}$, which can only be computed numerically. One might hope that the analytic expression would be a good approximation to the exact quantity, at least in some limit (say, for large mass). However, as observed in Ref. [1], this is not the case because $\langle\phi^2\rangle_{\mathrm{analytic}}$ contains a term which diverges logarithmically near a horizon unless the quantum scalar field is massless and conformally coupled. We have shown that, for a thermal state at the same temperature as the horizon, this divergence cancels with a divergence in $\langle\phi^2\rangle_{\mathrm{numeric}}$ near the horizon to give an overall finite quantity. In the literature other analytic approximations have been developed [10,11], some of which do not have this logarithmic divergence.

Unlike the Schwarzschild-de Sitter black hole [17], for lukewarm Reissner-Nordström–de Sitter black holes we have shown that a static quantum state can be constructed which has a regular renormalized expectation value $\langle\phi^2\rangle_{\mathrm{ren}}$ across both future and past event and cosmological horizons. This is the equivalent of the Hartle-Hawking state [12] for these black holes. This result is in accordance with the theorems of Kay and Wald [18], who proved that no regular thermal state can exist on a Reissner-Nordström-de Sitter black hole for which the temperatures of the event and cosmological horizons are not equal. When the temperatures do match, the fact that the region between the event and cosmological horizons has a regular Euclidean section [19] allows one to construct a thermal state at the natural temperature and then we have shown that this state has regular $\langle\phi^2\rangle_{\mathrm{ren}}$ on both the event and cosmological horizons.

Our work in this paper has considered only $\langle\phi^2\rangle_{\mathrm{ren}}$, and not the RSET. The computation of the RSET, following [1], mirrors that here for $\langle\phi^2\rangle_{\mathrm{ren}}$, but is considerably more complex. In particular, even though we have shown that $\langle\phi^2\rangle_{\mathrm{ren}}$ is finite on both the event and cosmological horizons, this does not guarantee that the RSET will be finite there. We plan to report on this in the near future.

[1] P. R. Anderson, W. A. Hiscock, and D. A. Samuel, Phys. Rev. Lett. **70**, 1739 (1993); Phys. Rev. D **51**, 4337 (1995).

[2] T. Elster, Classical Quantum Gravity **1**, 43 (1984); M. S. Fawcett, Commun. Math. Phys. **89**, 103 (1983); V. P. Frolov and A. I. Zelnikov, Phys. Lett. **115B**, 372 (1982); Phys. Rev. D **29**, 1057 (1984); P. B. Groves, P. R. Anderson, and E. D. Carlson, Phys. Rev. D **66**, 124017 (2002); K. W. Howard and P. Candelas, Phys. Rev. Lett. **53**, 403 (1984); B. P. Jensen, J. G. McLaughlin, and A. C. Ottewill, Phys. Rev. D **45**, 3002 (1992); **51**, 5676 (1995).

[3] K. W. Howard, Phys. Rev. D **30**, 2532 (1984).

[4] B. P. Jensen and A. C. Ottewill, Phys. Rev. D **39**, 1130 (1989).

[5] P. Candelas, Phys. Rev. D **21**, 2185 (1980).

[6] P. Candelas and K. W. Howard, Phys. Rev. D **29**, 1618 (1984); M. S. Fawcett and B. F. Whiting, in *Quantum Structure of Space and Time*, edited by M. J. Duff and C. J. Isham (Cambridge University Press, Cambridge, England, 1982).

[7] P. Candelas and B. Jensen, Phys. Rev. D **33**, 1596 (1986).

[8] P. R. Anderson, Phys. Rev. D **39**, 3785 (1989).

[9] A. DeBenedictis, Gen. Relativ. Gravit. **31**, 1549 (1999); V. P. Frolov, Phys. Rev. D **26**, 954 (1982); V. P. Frolov, in *Quantum Gravity*, edited by M. A. Markov and P. C. West (Plenum, New York, 1984).

[10] A. A. Popov, Phys. Rev. D **70**, 084047 (2004); S. V. Sushkov, Gravitation Cosmol. **6**, 45 (2000); Phys. Rev. D **62**, 064007 (2000).

[11] P. R. Anderson, E. Mottola, and R. Vaulin, arxiv:0707.3751; V. P. Frolov and A. I. Zelnikov, Phys. Rev. D **35**, 3031 (1987); J. Matyjasek, Acta Phys. Pol. B **27**, 2005 (1996); Classical Quantum Gravity **14**, L15 (1997); Phys. Rev. D **55**, 809 (1997); Acta Phys. Pol. B **30**, 971 (1999); Phys. Rev. D **59**, 044002 (1999); **61**, 124019 (2000); **71**, 027504 (2005); D. N. Page, Phys. Rev. D **25**, 1499 (1982); A. A. Popov, Phys. Rev. D **67**, 044021 (2003); T. Zannias, Phys. Rev. D **30**, 1161 (1984).

[12] J. Hartle and S. W. Hawking, Phys. Rev. D **13**, 2188 (1976).

[13] W. Unruh, Phys. Rev. D **14**, 870 (1976).

[14] D. Boulware, Phys. Rev. D **12**, 350 (1975).

[15] P. R. Anderson, Phys. Rev. D **41**, 1152 (1990).

[16] A. Satz, F. D. Mazzitelli, and E. Alvarez, Phys. Rev. D **71**, 064001 (2005).

[17] T. R. Choudhury and T. Padmanabhan, Gen. Relativ. Gravit. **39**, 1789 (2007); G. Denardo and E. Spallucci, Nuovo Cimento B **53**, 334 (1979); **55**, 97 (1980); W. A. Hiscock, Phys. Rev. D **39**, 1067 (1989); F.-L. Lin and C. Soo, Classical Quantum Gravity **16**, 551 (1999); D. Markovic and W. G. Unruh, Phys. Rev. D **43**, 332

(1991); T. Padmanabhan, Phys. Rep. **406**, 49 (2005); S. Tadaki and S. Takagi, Prog. Theor. Phys. **83**, 941 (1990).

[18] B. S. Kay and R. M. Wald, Phys. Rep. **207**, 49 (1991).

[19] F. Mellor and I. G. Moss, Classical Quantum Gravity **6**, 1379 (1989); Phys. Lett. B **222**, 361 (1989).

[20] L. J. Romans, Nucl. Phys. **B383**, 395 (1992).

[21] D. Morgan, S. D. Thom, E. Winstanley, and P. M. Young, Gen. Relativ. Gravit. **39**, 1719 (2007).

[22] E. Winstanley and P. M. Young (work in progress).

[23] H. Koyama, Y. Nambu, and A. Tomimatsu, Mod. Phys. Lett. A **15**, 815 (2000); A. Tomimatsu and H. Koyama, Phys. Rev. D **61**, 124010 (2000).

[24] D. Astefanesei, R. B. Mann, and E. Radu, J. High Energy Phys. 01 (2004) 029.

[25] F. G. Friedlander, *The Wave Equation on a Curved Space-*

Time (Cambridge University Press, Cambridge, England, 1976).

[26] Y. Decanini and A. Folacci, Phys. Rev. D **73**, 044027 (2006); arXiv:gr-qc/0512118.

[27] E. Poisson, Living Rev. Relativity **7**, 6 (2004); Classical Quantum Gravity **21**, R153 (2004).

[28] S. M. Christensen, Phys. Rev. D **14**, 2490 (1976); **17**, 946 (1978).

[29] W. Vetterling, W. Press, S. Teukolsky, and B. Flannery, *Numerical Recipes in FORTRAN* (Cambridge University Press, Cambridge, England, 1992).

[30] P. M. Young, Ph.D. thesis, University of Sheffield, 2006.

[31] M. Abramowitz and I. A. Stegun, *Handbook of Mathematical Functions* (Dover, New York, 1964).